# $T_h$-Symmetrical Hexakisadducts of $C_{60}$ with a Densely Packed π-Donor Shell Can Act as Energy- or Electron-Transducing Systems

**Michael Diekers,[b] Chuping Luo,[a] Dirk M. Guldi,*[a] and Andreas Hirsch*[b]**

*Dedicated to Professor Ortwin Brede on the occasion of his 60th birthday*

**Abstract:** For the first time several $T_h$-symmetrical hexakisadducts of $C_{60}$ bearing up to six electro- and photoactive *o*-phenylene diamine or 9,10-dialkoxyanthracene moieties were synthesized and subjected to photoinduced electron/energy-transfer studies. Both donors form a densely packed π-donor shell surrounding the fullerene core. In these novel core–shell ensembles (**7** and **19**), either an efficient energy transfer from the dialkoxyanthracene periphery, or an electron transfer from the *o*-phenylene diamine periphery transduces the flow of excited-state energy or electrons, respectively, to the fullerene moiety, which resides in the central core. Due to the relatively high reduction potential of the fullerene core, which is anodically shifted by ≈0.7 V, compared with that of pristine $C_{60}$, the outcome of these intramolecular reactions depends mainly on the donor ability of the peripheral system. Interestingly, the charge-separated state in the *o*-phenylene diamine heptad (**7**; $\tau = 2380$ ns in benzonitrile) is stabilized by a factor of 20 relative to the corresponding *o*-phenylene diamine dyad (**6**; $\tau = 120$ ns in benzonitrile), an effect that points unequivocally to the optimized storage of charges in this highly functionalized fullerene ensemble.

**Keywords:** donor–acceptor systems · electron transfer · fullerenes · nanostructures

## Introduction

Ever since the discovery of $C_{60}$, its aesthetically pleasing structure with perfect icosahedral symmetry, has held a deep fascination for chemists who construct architectures of higher complexity (i.e., core–shell structures, dendrimers, etc.).[1] Furthermore, the electron- and energy-acceptor properties of fullerenes stimulated a remarkable growth, which has led to a seemingly disparate field of studies. The delocalization of charges—electrons or holes—within the giant, spherical carbon framework (diameter > 7.5 Å) together with the rigid, confined structure of the aromatic π-sphere offer unique opportunities for stabilizing charged entities.[2] An impressive demonstration of this is the 24% efficient charge separation within a $C_{60}$-based molecular tetrad.[3] The lifetime of the spatially separated (≈49 Å) radical pair, a product of a sequence of energy- and electron-transfer reactions, reaches well beyond milliseconds (0.38 s) into a time domain which has never been accomplished so far in an artificial photosynthetic reaction center.

Consequently, the utilization of $C_{60}$-based materials in nanostructured devices, such as photoelectrochemical cells, that gives rise to efficient photocurrent generation, is currently at the forefront of intense investigation.[4] As far as injection of electrons into semiconducting electrodes is concerned, however, certain limitations of choosing this acceptor emerge. One of the biggest shortcomings is the low first one-electron reduction potential (≈ −0.9 V versus ferrocene) which, although rendering them good electron acceptors, limits the energy for injection into the electrode in molecular devices.[5] Ultimately, this limits the energy stored in the charge-separated state.

In the search for fullerene structures that enable us to address these issues (vide supra), we now report on the design of two novel $T_h$-hexakisadducts (**7** and **19**). The highly symmetric $T_h$-tecton facilitates loading of the fullerene core with a shell of up to six electron-donor moieties, which makes these systems particularly appealing for photoconversion processes. Although considerable attention has focused on the hexa-addition of fullerenes,[1, 6] addition of electron donors and/or chromophores and, thereby, the design of highly functional donor–acceptor model systems is rare so far. Placing six chromophores at the fullerene periphery enhances, for example, the light-collection and light-transduction features of the resulting core–shell ensembles. Ultimately this can lead to high solar energy conversion efficiencies, comparable with those seen in dendrimer structures.

[a] Dr. habil. D. M. Guldi, Dr. C. Luo
University of Notre Dame, Radiation Laboratory
Notre Dame, IN 46556 (USA)
Fax: (+1) 219-631-8068
E-mail: guldi.1@nd.edu

[b] Prof. Dr. A. Hirsch, Dipl.-Chem. M. Diekers
Institut für Organische Chemie
Universität Erlangen-Nürnberg
Henkestr. 42, 91054 Erlangen (Germany)
Fax: (+49) 9131-8522537
E-mail: hirsch@organik.uni-erlangen.de

  0947-6539/02/0804-0979 $ 17.50+.50/0 

3-Dimensional core–shell architectures are typically designed to bear an electro- and/or photoactive interior core, a sterically crowded, closed-packed shell, and a highly functional surface. Some of their most fascinating features extend to light-harvesting arrays and electron-transfer relays of different complexities (i.e., enhancing the molecular function with increasing generation).[7]

For the present study, *o*-phenylene diamine ($E_{1/2} = +0.232$ V versus ferrocene) and 9,10-dialkoxyanthracene ($E_{1/2} = +0.620$ V versus ferrocene) were chosen as electron-donating addends,[8] since the difference in their one-electron oxidation potentials helps to modulate the free energy changes, $-\Delta G^{\circ}_{ET}$. Both *o*-phenylene diamine and 9,10-dialkoxyanthracene create shells of densely packed π-donors surrounding the fullerene core, and thereby shield it quite well from the environment. In this paper, a detailed account of the photophysical properties is given, with particular focus on the electron- and energy-transduction processes.

## Results and Discussion

**Syntheses**: The design of a hexakisadduct containing six *o*-phenylenediamine addends is based on the fact that a sixfold addition of malonates by using the template mediation technique that we developed previously leads to adducts with a pseudo-octahedral $T_h$-symmetrical addition pattern with good yields and regioselectivities.[9] This approach requires the symmetrical incorporation of the *o*-phenylenediamine moiety into a cyclic malonate, since otherwise the overall symmetry of the resulting hexakisadduct would be lower than $T_h$, and a mixture of constitutional isomers would be obtained that would be difficult to separate. We therefore selected the cyclic malonate **1** as a suitable target addend, which was obtained by transformation of the dimethyl-*o*-phenylenediamine **2**[10] into the diol **3**[11] and subsequent coupling with malonyl dichloride (Scheme 1). The last step was carried out using very dilute solutions of the starting materials in order to prevent polymerization. For this purpose, a solution of malonyl dichloride in methylene chloride (8 mM) was slowly added (30 drops per min) to **3** (4 mM) in methylene chloride. In addition to the [1+1] macrocycle **1** the [2+2] and [3+3] rings **4** and **5** were formed simultaneously. The three cyclic malonates **1**, **4**, and **5** were formed in a 10:8:1 ratio with an overall yield of 30%. After isolation by preparative HPLC all three macrocycles were completely characterized. As expected, the NMR spectra of **1**, **4**, and **5** are qualitatively the same, since the cyclic oligomers contain the same number of magnetically inequivalent sets of H and C atoms.

To test whether the monomalonate **1** was suitable for nucleophilic cyclopropanations, we first synthesized the monoadduct **6** by allowing **1** to react with $C_{60}$ in the presence of $CBr_4$ and DBU (diazabicycloundecane, Scheme 2). After purification by flash chromatography using a mixture of toluene and triethylamine as eluent, **6** was obtained in 23% yield. The spectroscopic characterization of monoadduct **6** is consistent with the depicted structure.

Subsequently, hexakisadduct **7** was synthesized in 12% isolated yield using the reversible template mediation methodology (Scheme 3). For this purpose, $C_{60}$ was treated with a tenfold excess of malonate **1** in the presence of 9,10-dimethylanthracene (DMA) and $CBr_4$/DBU. Isolation of **7** was accomplished by flash chromatography followed by preparative HPLC. Compound **7** has the typical spectroscopic fea-

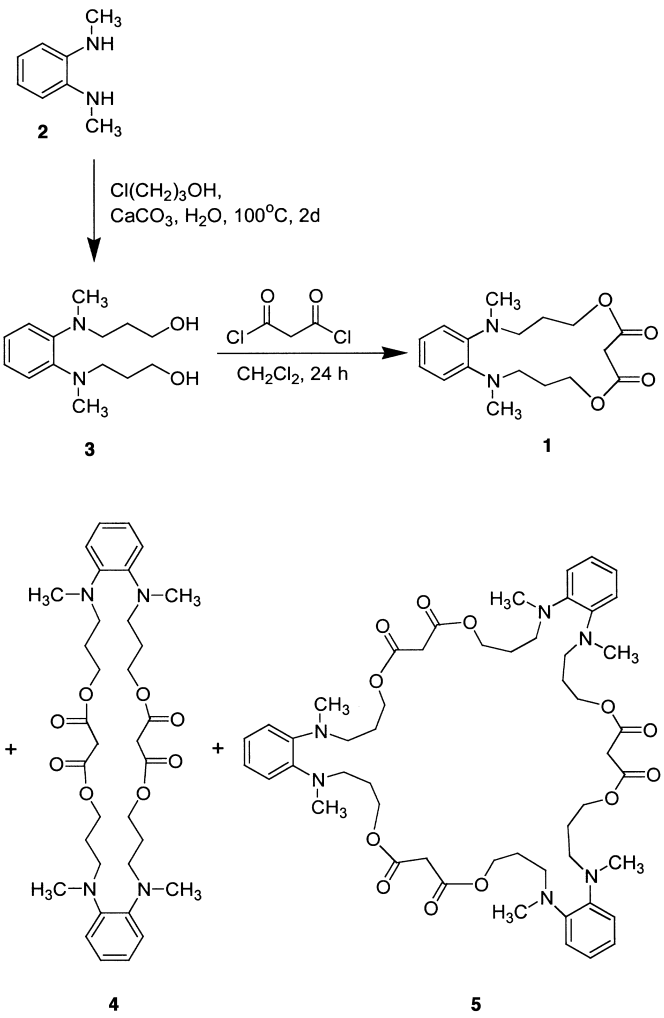


2 3 1 4 5

Scheme 1. Formation of cyclic malonate **1** by transformation of the dimethyl-*o*-phenylenediamine **2** into the diol **3** followed by coupling with malonyl dichloride.

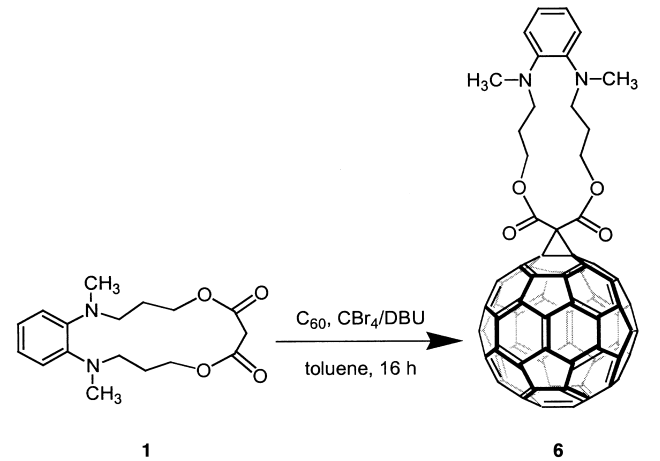


1 6

Scheme 2. Synthesis of the monoadduct **6** by the reaction of **1** with $C_{60}$ in the presence of $CBr_4$ and DBU.



0947-6539/02/0804-0980 $ 17.50+.50/0 *Chem. Eur. J.* **2002**, *8*, No. 4

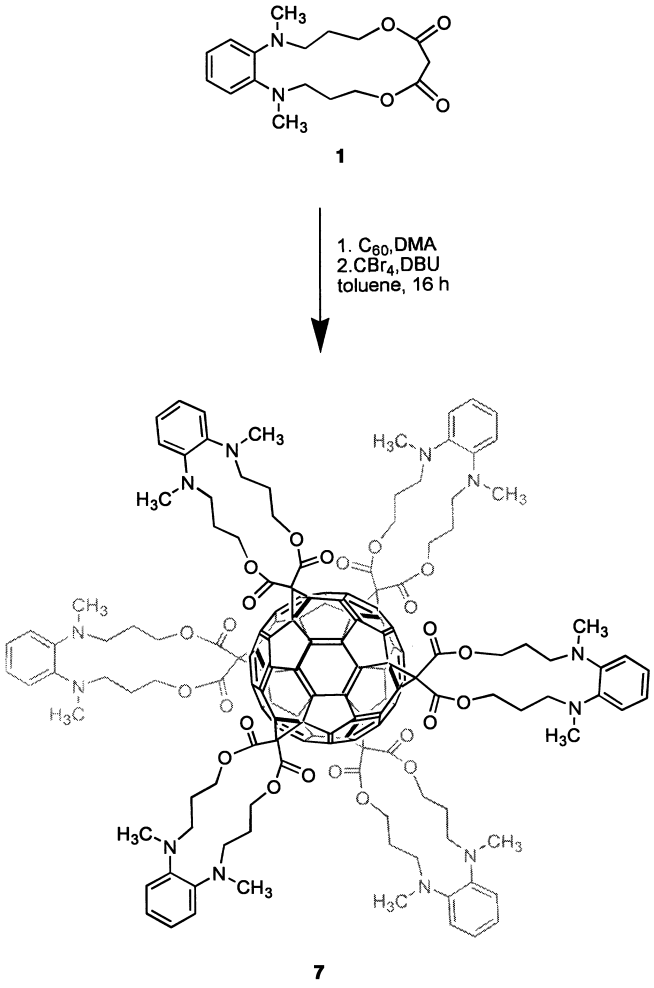


Scheme 3. Synthesis of hexakisadduct **7** by using the reversible template mediation methodology.

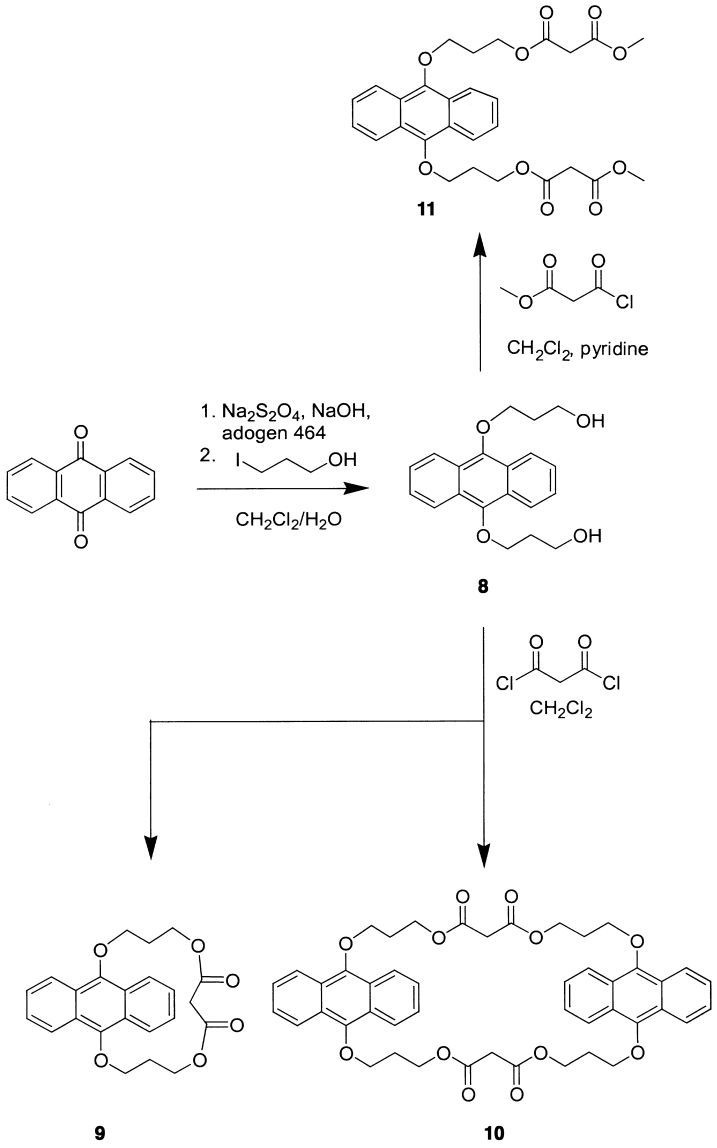


Scheme 4. Formation of diol **8** and compounds **9** and **10**.

tures commonly observed for $T_h$-symmetrical hexakisadducts. For example, in the $^{13}C$ NMR spectrum only two signals appear for the $sp^2$- and one signal for the $sp^3$-C atoms of the fullerene cage at $\delta = 140.9$, 145.7, and 69.0, respectively. The FAB mass spectrum displays the molecular ion peak at $m/z =$ 2630, and the UV/Vis spectrum of the yellow compound **7** shows the typical structure, with the most intensive absorptions at $\lambda_{max} = 239$ and 270 nm.

In order to synthesize new donor–acceptor systems, we decided to use the anthracene moiety, which is more difficult to oxidize than the *o*-phenylene diamine unit. As starting material we used anthraquinone, which was reduced, and subsequently hydroxyalkylated to give the diol **8** (Scheme 4). In analogy to diol **3**, which we have also previously transformed into a bismalonate by allowing it to react with methyl malonyl chloride,[12] we used **8** to synthesize both the cyclic monomalonate **9** and the open chain bismalonate **11** (Scheme 4).[13] As in the *o*-phenylenediamine case, the formation of the [1+1] macrocycle **9** is accompanied by that of the [2+2] ring **10**, even though the reaction was carried out under high dilution conditions. Compounds **9** and **10** were formed in a 3:2 ratio in an overall yield of 23 %. Isolation was achieved by flash chromatography using a toluene/ethyl acetate mixture as eluent.

The bifunctional donor **11** should be a suitable addend for a tether functionalization of $C_{60}$. The corresponding cyclopropanation reaction afforded a mixture of the monoadduct **12**, the bisadducts **13**–**15**, and the dimer **16** in yields of 23 %, 5 %, 9 %, 3 %, and 3 %, respectively (Scheme 5). The purification of **12** was achieved by flash chromatography. The bisadducts and the dimer were subsequently isolated by preparative HPLC. Whereas the characterization of the monoadduct **12** and the dimer **16** was straightforward, the structure assignment of the bisadducts **13**–**15** required careful evaluation of the spectroscopic and computational data and comparison of their electronic absorption spectra with those reported for related regioisomeric bisadducts.[1a, 14] In principle, over and above to the seven bisaddition patterns (*cis*-2, *cis*-3, *e*, *trans*-4, *trans*-3, *trans*-2, *trans*-1) that can be achieved by two malonate addends, "in–out" geometrical isomers of the resulting cyclopropane rings also have to be considered. However, due to steric restrictions only *out*–*out* isomers are possible. As a consequence, since **14** has $C_1$ symmetry (NMR), it must

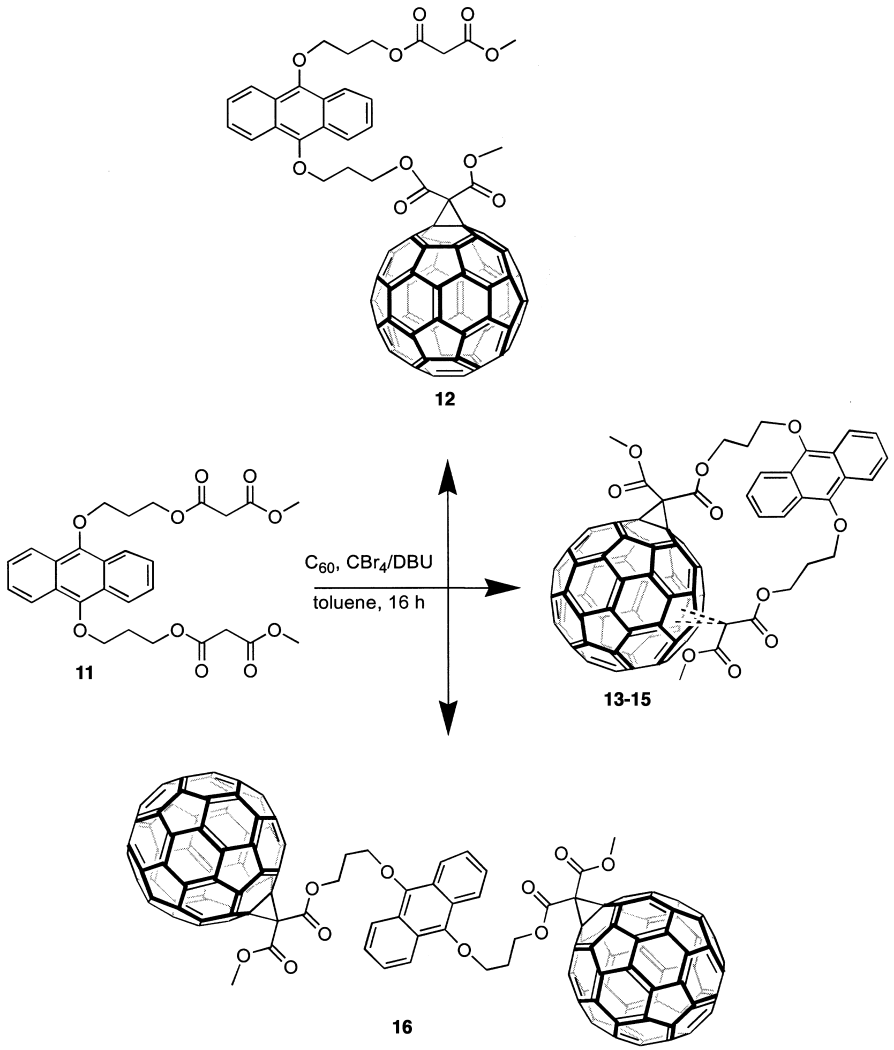


Scheme 5. Cyclopropanation to give a mixture of the monoadduct **12**, the bisadducts **13**–**15**, and the dimer **16**.

be the *e*-isomer. The $^{13}C$ NMR spectra of the bisadducts **13** and **15** reveal $C_2$ symmetry. Evaluation of the UV/Vis spectra as well as energy calculations (PM3) allow **13** to be assigned as the *cis*-3 isomer and **15** as the *trans*-3 isomer.

Although anthracene derivatives are known to undergo [4+2] cycloadditions with the [6,6]-bonds of $C_{60}$ no indication for the formation of the corresponding side products is found. This is very likely to be due to the fact that here the [4+2] cycloaddition is highly reversible, and that the retro-reaction occurs under the conditions of the purification.

Treatment of **9** with $C_{60}$ under typical monocyclopropanation conditions afforded the monoadduct **17** in 32% yield (Scheme 6). Subsequent addition of five diethylmalonyl addends to the octahedral sites by using the template mediation method led to the mixed hexakisadduct **18** in 23% yield (Scheme 6). The unambiguous structural assignment of these dyads was accomplished by NMR, IR, and UV/Vis spectroscopy, and FAB mass spectrometry.

The synthesis of the hexakisadduct **19** was again carried out starting directly from $C_{60}$ and using the reversible template mediation methodology (Scheme 7). The poor solubility of this interesting fullerene derivative, which carries covalently bound addends that completely cover the spherical core with the unsaturated π-systems of the planar anthracene building blocks, makes the workup more difficult than in the case of **7**. However, we succeeded in the isolation of **19** by applying a pre-purification using flash chromatography, through which a mixture of pentakis- and hexakisadducts was obtained. After preparative HPLC over a Nucleosil stationary phase using a mixture of methylene chloride and 0.3% ethanol, **19** was obtained in 9% yield. Due to the poor solubility of **19**, NMR spectroscopy had to be carried out in tetrachloroethane at 80 °C. The $^{13}C$ NMR spectrum shows the typical resonances at $\delta = 69.5$ for the magnetically equivalent $sp^3$-C atoms of the fullerene cage and at $\delta = 140.3$ and 144.6 for the two types of cluster $sp^2$-C atoms. Because the absorption spectra of the dyads are simple superpositions of those of the individual units, the UV/Vis spectrum of hexakisadduct **19** is dominated by the six anthracene units. It shows a strong absorption at $\lambda_{max} = 264$ nm and a triple absorption at $\lambda_{max} = 370$, 389, and 411 nm, which is typical for the anthracene moiety.

**Photophysics**: Two important features of $T_h$-hexakisadducts, which are expected to have a major effect on the electron-transfer dynamics in core–shell structures **7**, **18**, and **19**, should be discussed with reference to the well-studied fullerene monoadducts (see for example **6**, **12**, and **17**). First, the reduction potential shifts anodically from about −1.1 V for the monoadduct to −1.69 V (versus ferrocene) in the corresponding $T_h$-hexakisadduct.[5, 15] In addition, the one-electron reduction step is accompanied by an inherent loss of reversibility. The second feature is the fullerene singlet excited-state energy, which is altered in favor of an electron transfer (vide infra). The corresponding energies result in a strong blue shift from 1.76 to 1.89 eV in the mono- versus the hexakisadduct.

In the donor–acceptor ensemble **19** the absorption features of the anthracenoid moieties, with a 6:1 molecular ratio, direct the 410 nm excitation exclusively to the periphery.[16] The anthracene fluorescence, which has a quantum yield ($\Phi$) of 0.87, is subject to a quantitative emission quenching ($\Phi = 1.1 \times 10^{-3}$) in toluene (Figure 1a). In addition to the 460 nm anthracene emission, the familiar fullerene fluorescence was found with a *0–0 emission at 660 nm



0947-6539/02/0804-0982 $ 17.50+.50/0 *Chem. Eur. J.* **2002**, *8*, No. 4

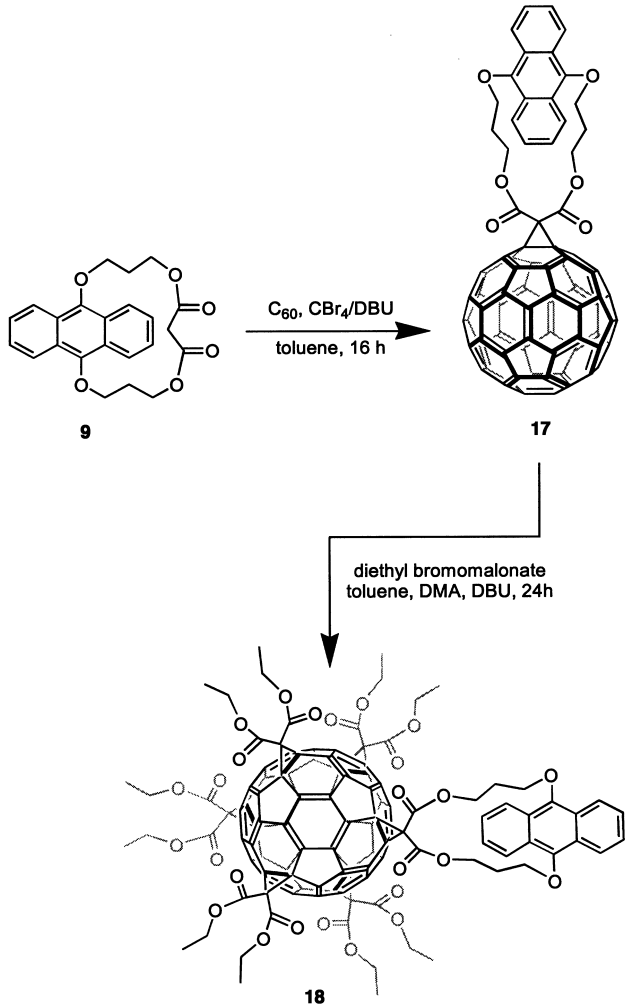


Scheme 6. Reaction of **9** with $C_{60}$ to produce monoadduct **17**.

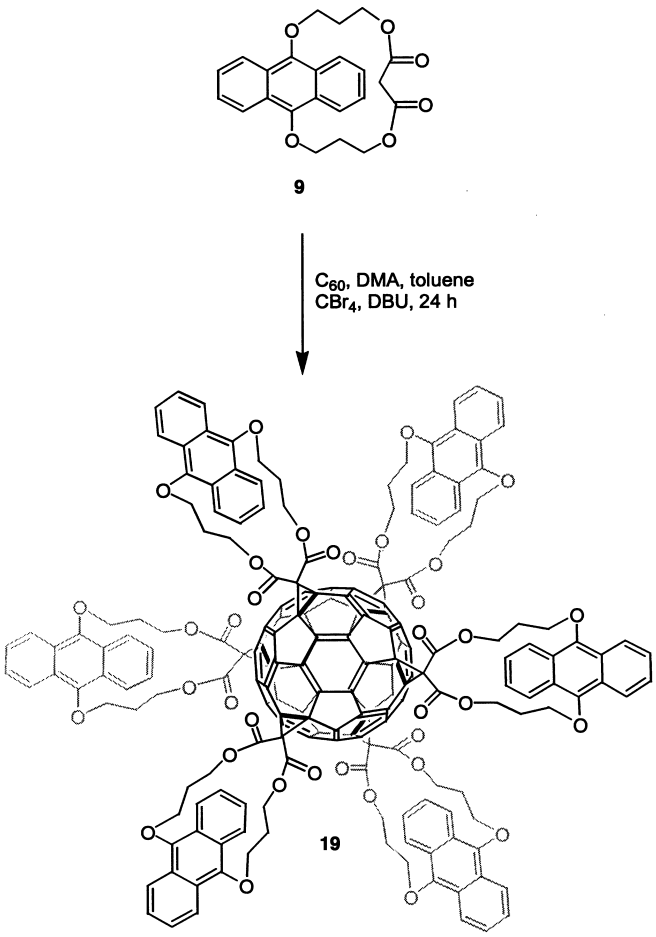


Scheme 7. Synthesis of the hexakisadduct **19** from $C_{60}$ by using the reversible template mediation methodology.

(Figure 1b). This occurs, despite the near exclusive excitation at 410 nm of the anthracenoid moieties. It is important to note that the emission pattern of the anthracenoid units remains unchanged and is not affected by the presence of the fullerene core. To probe the mechanism of producing the fullerene emission, an excitation spectrum of the 660 nm emission was taken (Figure 1a). In fact, the excitation spectrum of **19** is an excellent match with that of a 9,10-dialkoxy-anthracene model (**9**) and it also resembles the 411 nm ground-state maximum of **9**. This serves as sound support for the hypothesis that the origin of the excited-state energy is the anthracenoid systems. By employing reference $\boldsymbol{T_h}$-$\mathbf{C_{66}(COOEt)_{12}}$ ($\Phi = 1.09 \times 10^{-3}$), with matching absorption at the 411 nm excitation wavelength, the fullerene fluorescence quantum yields were determined for core–shell ensemble **19**: in toluene, a $\Phi$ value of $5.5 \times 10^{-4}$ corresponds to only 51 % of that measured for reference $\boldsymbol{T_h}$-$\mathbf{C_{66}(COOEt)_{12}}$.

From the fluorescence quantum yield ($\Phi$) and the fluorescence lifetime ($\tau = 14.7$ ns) of reference **9**, the rate constant ($k = 5.4 \times 10^{10}\ s^{-1}$) of the intramolecular singlet–singlet energy transfer in **19** was derived according to the following expression [Eq. (1)].

$$k = [\Phi(\mathbf{9}) - \Phi(\mathbf{19})]/[\tau(\mathbf{9})\ \Phi(\mathbf{19})] \quad (1)$$

Since the results of the emission studies along with the thermodynamic calculations (vide infra) suggest that an intramolecular singlet–singlet energy transfer occurs from the outer shell to the inner core, further examination of this fullerene-based hybrid was deemed necessary. This led us to characterize the photophysics of **19** by means of time-resolved transient absorption spectroscopy. Following the initial transfer of singlet excited-state energy, which is completed within the first 20 ps (i.e., instrumental resolution), the fullerene singlet–singlet transitions were seen with $\lambda_{max}$ at 530, 780, and 860 nm (Figure 2a; 50 ps time delay). The fullerene singlet excited state deactivates by means of a spin-forbidden intersystem crossing[2e, 17] with a rate of $5.7 \times 10^8\ s^{-1}$ (Figure 2b) to produce the corresponding triplet manifold.

The differential absorption changes, recorded immediately after an 8 ns pulse, showed the same spectral features of the fullerene triplet excited state as observed at the end of the picosecond experiments (Figure 2a; 5000 ps time delay). To be precise, a maximum located at 590 nm (Figure 3) was observed in good agreement with the features recorded for $\boldsymbol{T_h}$-$\mathbf{C_{66}(COOEt)_{12}}$, and the fullerene triplet lifetime was estimated to be $\approx$85 μs. Similar to the fluorescence measurements (vide supra), the relative triplet quantum yield of **19** is $\approx$48 %, compared with $\boldsymbol{T_h}$-$\mathbf{C_{66}(COOEt)_{12}}$. Thus, our analysis

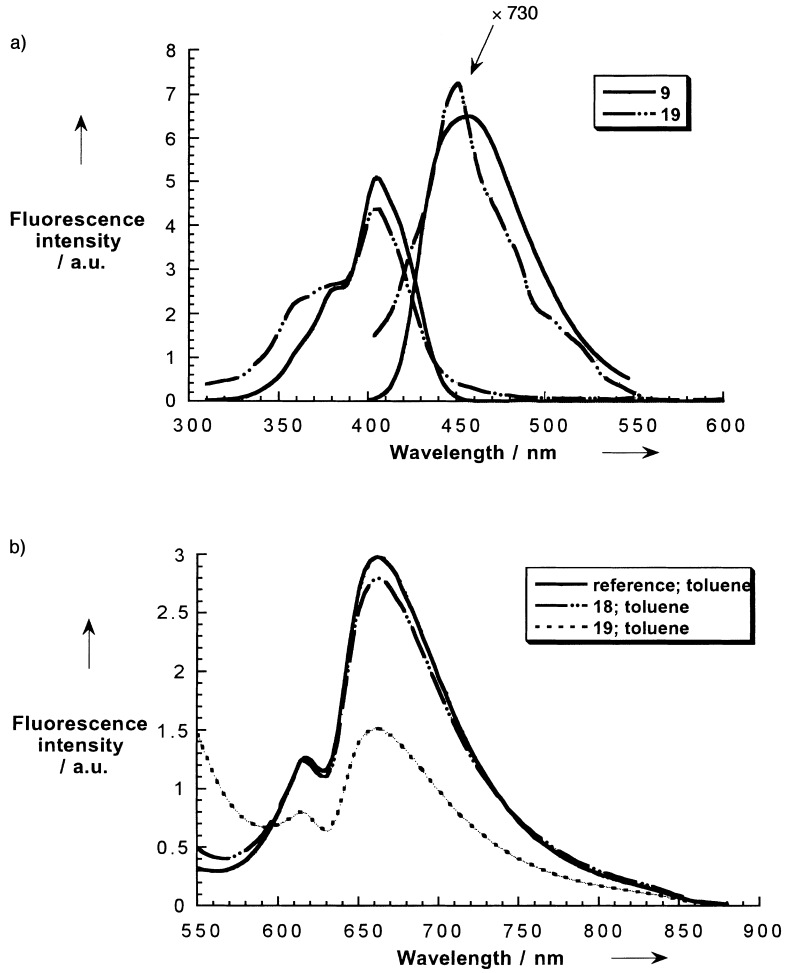


Figure 1. a) Emission spectra of **9** (solid line) and **19** (dashed line) in toluene with matching absorption at the 410 nm excitation wavelength (i.e., $OD_{410\,nm} = 0.7$) monitoring the anthracenoid moieties emission at 460 nm. Excitation spectra (normalized to exhibit matching signals $\approx 400$ nm) of **9** (solid line; 460 nm emission) and **19** (dashed line; 660 nm emission) in toluene; b) Emission spectra of $T_h$-**$C_{66}$(COOEt)$_{12}$** reference, **18**, and **19** in toluene with matching absorption at the 410 nm excitation wavelength (i.e., $OD_{410\,nm} = 0.7$) monitoring the fullerene emission at 660 nm.

shows the photosensitization effect of the anthracenoid chromophores, which act as an antenna shell and transmit their excited-state energy to the central fullerene core.

A conceivable rationale for the moderate transfer efficiency of $\approx 50\,\%$ is that the chromophore units at the periphery may be subject to interchromophore deactivations, and that, therefore, some of the excitation energy fails to reach the central fullerene core. To further substantiate this working hypothesis, the efficiency of another hexakisadduct (**18**), which carries only a single anthracenoid moiety, was examined and compared with that of **19**. In this case, the anthracenoid emission is further quenched ($\Phi = 4.1 \times 10^{-4}$). Most significantly, the fullerene emission quantum yield in **18** ($\Phi = 1.04 \times 10^{-3}$) matches that seen for fullerene reference $T_h$-**$C_{66}$(COOEt)$_{12}$** ($\Phi = 1.09 \times 10^{-3}$, Figure 1b).

The conclusion of the photophysical experiments, conducted with **18** and **19**, infers that an efficient intramolecular transfer of singlet excited-state energy from the periphery to the core prevails. This relates predominantly to the fact that the largest energy gap opens between the two singlet excited states ($-\Delta G^{o}_{ENT} \approx 0.8$ eV), namely, that of the anthracenoid and that of the fullerene. In turn, the endothermic electron transfer ($-\Delta G^{o}_{ET} \approx -0.2$ eV) plays, at the very best, a minor role. To activate an intramolecular electron transfer in a $C_{60}$-based core–shell system rather than an energy transfer, it was deemed necessary to select a better electron donor and/or to excite the fullerene core. These requisites are given in donor–acceptor ensemble **7** employing an *o*-phenylene diamine donor.

As a suitable model system for **7** we investigated first monoadduct **6**. Relative to the fluorescence of a **$C_{61}$(COOEt)$_2$** reference ($\lambda_{max} = 700$ nm; $\Phi = 6.0 \times 10^{-4}$),[2e, 17] the fullerene emission in **6** is markedly quenched and, more importantly, subject to solvent dependence. In particular, a noticeable decrease of the fluorescence—from *n*-chlorobutane ($\varepsilon = 7.39$) to DMF ($\varepsilon = 36.7$)—is deduced from the data summarized in Table 1 and Figure 4.[18] The observed trend can be interpreted as a first indication of an electron-transfer mechanism being responsible for the rapid deactivation of the fullerene singlet excited state. An alternative mechanism, namely, an intramolecular energy transfer from the fullerene singlet excited state ($E_{singlet} = 1.76$ eV) to the *o*-phenylene diamine moiety ($E_{singlet} = 3.97$ eV; $E_{triplet} = 3.08$ eV)[19] can be ruled out, based on the unfavorable thermodynamics.

To unravel the mechanism by which the fullerene singlet excited state in dyad **6** is deactivated, the transient absorption changes were recorded with several time delays after a short 18 ps laser pulse (355 nm). At short times (i.e., 50–100 ps), they are practically identical to those of a monoadduct reference (**$C_{61}$(COOEt)$_2$**) with a singlet–singlet absorption around 900 nm (Figure 5a). It is not the slow intersystem crossing dynamics ($7.4 \times 10^8\ s^{-1}$),[2e, 17] which govern the lifetime of the singlet excited state, but a rapid intramolecular decay of the singlet–singlet transition (THF: $1.3 \times 10^9\ s^{-1}$; Figure 5b). Here, the singlet lifetimes are strongly reduced, especially in solvents of high polarity. An illustration is given in Table 1, which displays the most relevant photophysical properties of **6**.

The transient absorption changes, recorded at the conclusion of this fast deactivation, are not superimposable with those recorded for the fullerene model (**$C_{61}$(COOEt)$_2$**), that is,



0947-6539/02/0804-0984 $ 17.50+.50/0 *Chem. Eur. J.* **2002**, *8*, No. 4

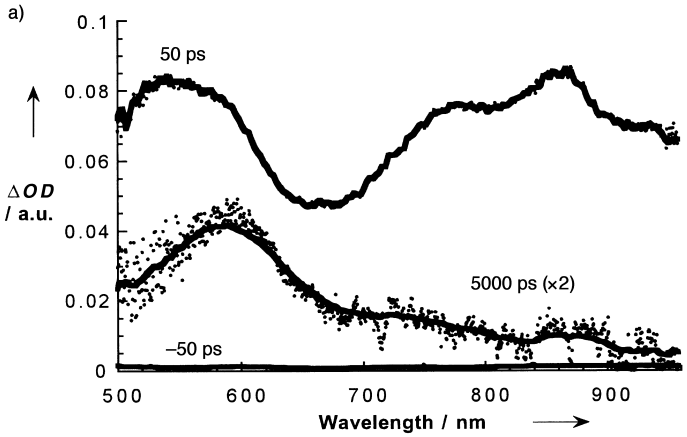


Figure 2. Differential absorption spectra obtained upon picosecond flash photolysis (355 nm) of $\approx 1.0 \times 10^{-5}$ M solutions of **19** in nitrogen-saturated toluene with a time delay of a) – 50 ps, 50 ps, and 5000 ps; b) Time-absorption profiles at 860 nm monitoring the fullerene ISC dynamics in **19**.

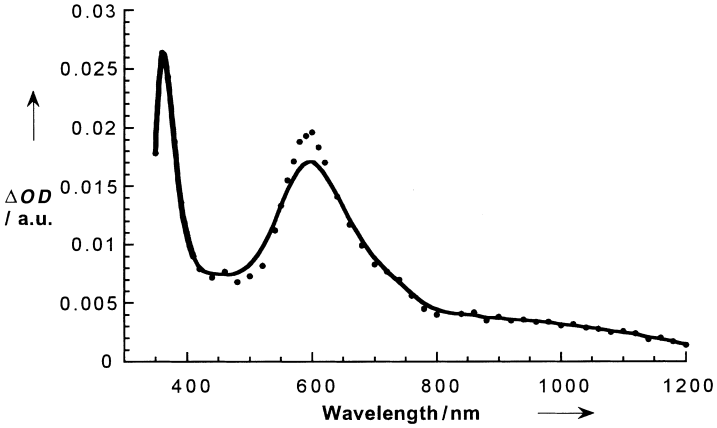


Figure 3. Differential absorption spectra (UV/Visible and near-infrared) obtained upon nanosecond flash photolysis (337 nm) of $\approx 1.0 \times 10^{-5}$ M solutions of **19** in nitrogen-saturated toluene with a time delay of 50 ns at room temperature.

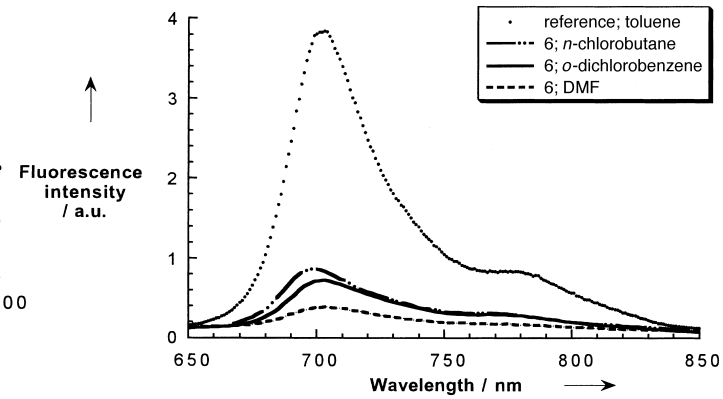


Figure 4. Emission spectra of $\mathbf{C_{61}(COOEt)_2}$ reference in toluene and dyad **6** in different solvents with matching absorption at the 310 nm excitation wavelength (i.e., $OD_{310\,nm} = 0.8$).

the fullerene triplet excited state (see Figure 5a; 4000 ps time delay). The fullerene triplet reveals two maxima: one in the visible region around 380 nm and one in the near-infrared region at 720 nm. Instead, the newly formed species shows a sharp peak around 1030 nm, the characteristic fingerprint of the one-electron reduced fullerene π-radical anion (Figure 6).[2e, 17] As far as the *o*-phenylene diamine moiety is concerned, a transient maximum in the visible region around 500 nm corroborates the oxidation of the donor and completes the characterization of the charge-separated radical pair.

Both fingerprints (i.e., 500 and 1030 nm) were employed as reliable probes to determine the lifetime of the associated charge-separated state and the overall quantum yield of the charge-separation process (see Table 1). The decay curves closely fit a single exponential decay component. In particular, lifetimes of the order of 100 nanoseconds were derived from the decay curves of the oxidized donor and reduced acceptor absorption at 500 nm and 1030 nm, respectively. Additional evidence for an intramolecular charge recombination comes from a set of experiments conducted with different laser power and different dyad concentrations:

Table 1. Some selected photophysical properties of dyad **6**.

| Solvent | $\varepsilon$ | $\Delta G_S$ [eV][a] | $-\Delta G^0_{ET}$ [eV][a] | $-\Delta G^0_{BET}$ [eV][a] | Lifetime ($\tau$); Singlet Excited State [ns] | Quantum Yield ($\Phi$); Fluorescence | Lifetime ($\tau$); Fluorescence [ns] | Lifetime ($\tau$); Radical Pair [ns] | Quantum Yield ($\Phi$); Radical Pair[b] |
|---|---|---|---|---|---|---|---|---|---|
| *n*-chlorobutane | 7.39 | – 0.2 | 0.45 | 1.3 | 0.81 | $1.5 \times 10^{-4}$ | 0.85 | | 0.71 |
| THF | 7.6 | – 0.21 | 0.65 | 1.1 | 0.76 | $1.3 \times 10^{-4}$ | 0.81 | 89 | |
| dichlorobenzene | 9.98 | – 0.33 | 0.75 | 1.0 | 0.54 | $1.2 \times 10^{-4}$ | 0.67 | 105 | 0.78 |
| benzonitrile | 24.8 | – 0.55 | 0.97 | 0.79 | 0.43 | $1.0 \times 10^{-4}$ | 0.53 | 120 | 0.86 |
| DMF | 36.7 | – 0.59 | 1.02 | 0.74 | 0.25 | $0.85 \times 10^{-4}$ | 0.34 | 130 | 0.49 |

[a] See for details reference [24]. $R_-$ (radius acceptor) = 3.6 Å; $R_+$ (radius donor) = 1.85 Å; $R_{DA}$ (donor – acceptor separation) = 5.8 Å. [b] Measured by the comparative technique using the fullerene triplet characteristics as reference.

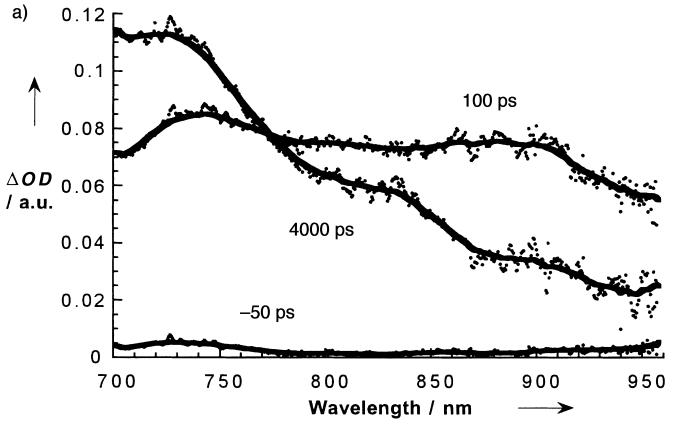


Figure 5. Differential absorption spectra obtained upon picosecond flash photolysis (355 nm) of $\approx 1.0 \times 10^{-5}$ M solutions of $\mathbf{C_{61}(COOEt)_2}$ reference in nitrogen-saturated toluene with a time delay of a) −50 ps, 100 ps, and 4000 ps; b) Time-absorption profiles at 900 nm of $\mathbf{C_{61}(COOEt)_2}$ reference in toluene and dyad **6** in THF and DMF monitoring the fullerene singlet–singlet decay. decreasing the radical-pair concentration in various increments by up to 65% failed to lead to any notable changes in the charge-recombination kinetics.

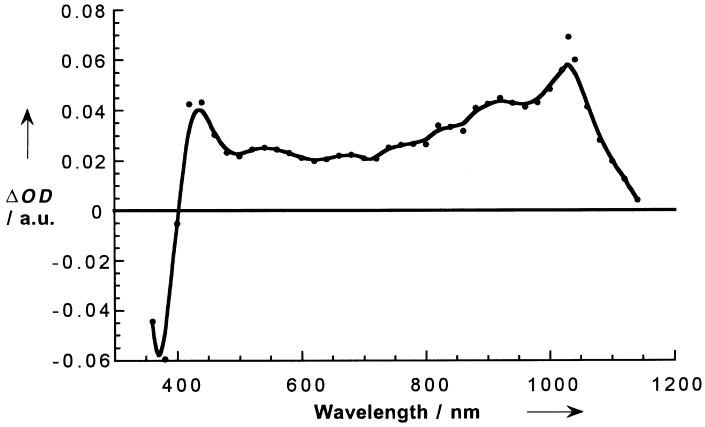


Figure 6. Differential absorption spectra (UV/Visible and near-infrared) obtained upon nanosecond flash photolysis (337 nm) of $\approx 1.0 \times 10^{-5}$ M solutions of dyad **6** in nitrogen-saturated benzonitrile with a time delay of 50 ns at room temperature.

The choice of the strong *o*-phenylene diamine donor ($E_{1/2} = +0.232$ V versus ferrocene) led in dyad **6** to the activation of an electron transfer. Encouraged by this observation, we focussed on core–shell ensemble **7**. In toluene, *n*-chlorobutane, and THF, the endothermic and marginally exothermic free energy changes for an intramolecular electron transfer ($-\Delta G^{\circ}_{ET} \leq 0.04$ eV) suggest the absence of an efficient electron transfer in photoexcited **7**. Indeed, the features linked to the fullerene singlet excited state clearly lack any solvent dependence in their decay (Table 2). Furthermore, in the nanosecond experiments, just the long-lived triplet–triplet characteristics ($\lambda_{max} = 590$ nm) were found to a reasonably high extent (similar to Figure 2). In comparison with dyad **6**, the lack of electron transfer relates mainly to the anodically shifted reduction potential of the fullerene core (vide supra).

Different behavior was observed in more polar solvents: the choice of benzonitrile or DMF results in a much stronger exothermicity of the electron transfer (i.e., $-\Delta G^{\circ}_{ET}$ values $\approx 0.5$ eV). The fluorescence properties of **7**, that is, fluorescence quantum yield and fluorescence lifetime, now reveal quenching with a marked solvent dependence that starts with THF and ranges to DMF (Table 2). From these characteristics we infer that an intramolecular electron transfer in core–shell ensemble **7** is, indeed, activated in benzonitrile and likewise in DMF.

Definitive evidence in support of this hypothesis was found in transient absorption spectroscopy. On the 50 ps timescale, the typical fullerene singlet–singlet absorption with maxima at 530, 780, and 860 nm can still be seen (similar to Figure 2; 50 ps time delay). Instead of the slow intersystem crossing dynamics ($5.7 \times 10^8$ s$^{-1}$) and the concomitant increase of the triplet–triplet absorption $\approx 590$ nm, a rapid decay of the singlet–singlet absorption was noticed. More important is the fact that the differential absorption changes of **7** in benzonitrile, noted at the end of the singlet excited-state decay, are strikingly different from the triplet excited-state features (compare Figure 7 and Figure 3). Additional pulse radiolytic reduction experiments allowed us to attribute the newly formed transient to a charge-separated state with a fullerene

Table 2. Some selected photophysical properties of core–shell ensemble **7**.

| Solvent | $\varepsilon$ | $\Delta G_S$ [eV][a] | $-\Delta G^{\circ}_{ET}$ [eV][a] | $-\Delta G^{\circ}_{BET}$ [eV][a] | Lifetime ($\tau$); Singlet Excited State [ns] | Quantum Yield ($\Phi$); Fluorescence | Lifetime ($\tau$); Fluorescence [ns] | Product | Lifetime ($\tau$); Radical Pair [ns] |
|---|---|---|---|---|---|---|---|---|---|
| toluene | 2.39 | 1.2 | −1.14 | | 0.64 | $3.1 \times 10^{-4}$ | 1.14 | triplet | |
| *n*-chlorobutane | 7.39 | −0.2 | 0.03 | | 0.62 | $3.9 \times 10^{-4}$ | 1.02 | triplet | |
| THF | 7.6 | −0.21 | 0.04 | | 0.62 | $3.9 \times 10^{-4}$ | 0.98 | triplet | |
| benzonitrile | 24.8 | −0.55 | 0.45 | 1.44 | 0.36 | $2.1 \times 10^{-4}$ | 0.36 | radical pair | 2380 |
| DMF | 36.7 | −0.59 | 0.51 | 1.39 | 0.27 | $1.7 \times 10^{-4}$ | 0.27 | radical pair | 1050 |

[a] See for details reference [24]. $R_-$ (radius acceptor) = 3.6 Å; $R_+$ (radius donor) = 1.85 Å; $R_{DA}$ (donor–acceptor separation) = 5.8 Å.



0947-6539/02/0804-0986 $ 17.50+.50/0 *Chem. Eur. J.* **2002**, *8*, No. 4

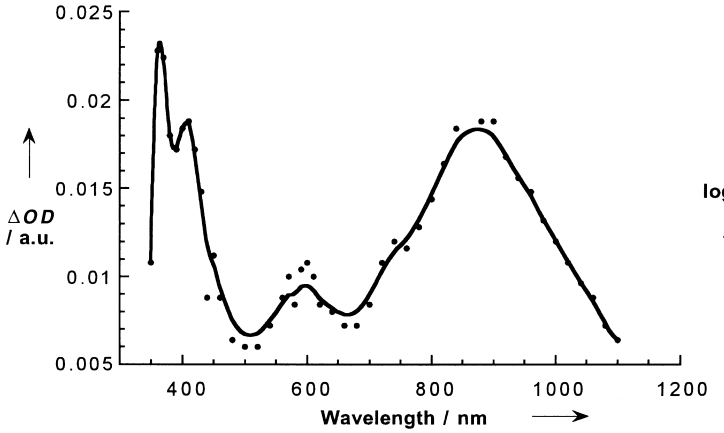


Figure 7. Differential absorption spectra (UV/Visible and near-infrared) obtained upon nanosecond flash photolysis (337 nm) of $\approx 1.0 \times 10^{-5}$ M solutions of **7** in nitrogen-saturated benzonitrile with a time delay of 50 ns at room temperature.

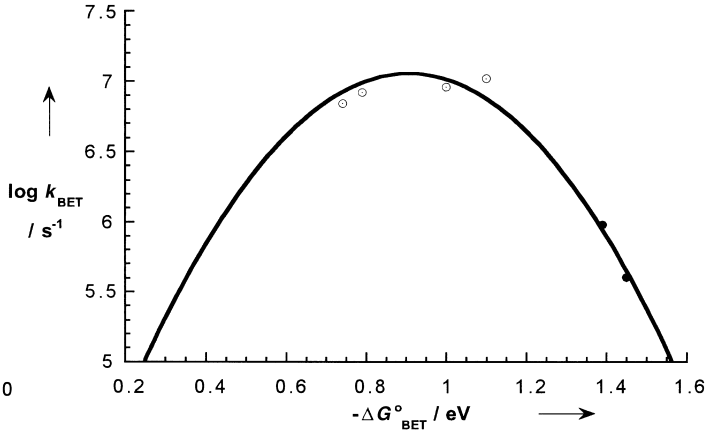


Figure 8. Driving-force ($-\Delta G^{\circ}_{BET}$) dependence of intramolecular charge-recombination rate constants in dyad **6** (white circles) and in **7** (black circles). The line represents the best fit ($\lambda = 0.89$ eV and $V = 0.22$ cm$^{-1}$).

π-radical anion absorption (≈900 nm).[20] Complementary nanosecond experiments give rise to lifetimes ($\tau$) of 2.38 μs and 1.05 μs in benzonitrile and DMF, respectively. The charge recombination processes obey in both cases a first-order rate law and lead to a complete recovery of the singlet ground state.

The lifetimes of the charge-separated states can be correlated with the solvent polarity. The dependence of $k_{BET}$ ($\tau = 1/k_{BET}$) versus free energy changes (Table 2) indicates stabilizing effects for the charge-separated state at higher $-\Delta G^{\circ}_{BET}$ values in core–shell ensemble **7**. These are clear attributes of the "Marcus-inverted" region, the highly exergonic region ($-\Delta G^{\circ} > \lambda$), where the electron-transfer rates start to decrease with increasing free energy changes.[21] In contrast, the lifetime of the radical pair in dyad **6** grows gradually from the moderately to the strongly polar solvents, and this indicates that these rates are in the "Marcus-normal" region (Table 1). In general, the driving forces of the charge-recombination processes in **7** (≈1.4 eV) are markedly larger than those in **6** (0.74–1.1 eV), which support the above assignment regarding the charge-recombination kinetics being either in the "Marcus-inverted" or "Marcus-normal" region.

To quantify the driving-force dependence on the rate constants ($k_{ET}$), the semi-classical Marcus equation was employed.[22] Figure 8 shows the log $k_{BET}$ versus $-\Delta G^{\circ}_{BET}$ plot for the different donor–acceptor ensembles. From the best fits of the driving-force dependence on ET rates, the following values for the reorganization energies ($\lambda$) and electronic couplings ($V$) were derived: $\lambda = 0.89$ eV and $V = 0.22$ cm$^{-1}$. The reorganization energy is smaller than those reported previously for porphyrin–quinone and zinc porphyrin–free-base porphyrin-linked systems, which are typically in the range between 0.8 and 1.2 eV,[22] but larger than in a zinc tetraphenylporphyrin–fullerene dyad (0.67 eV).[23]

## Conclusion

In summary, we demonstrated that core–shell ensembles **7** and **19** function as energy- and electron-transducer systems, transmitting electrons and singlet excited-state energy, respectively, to the redox- and photoactive $T_h$-hexakisadduct core.

Photoinduced electron transfer, in the core shell ensemble **7**, generates a remarkably long-lived charge-separated state ($\tau = 2380$ ns in benzonitrile). Its energy (1.44 eV) is notably higher than that in the analogous mono- and bis-adducts (0.79 eV).[12] This shifts the back electron transfer in **7** far into the "Marcus-inverted" region, which, at least in part, decelerates the energy-wasting charge recombination. Of apparently equal importance is the interruption of the fullerene π-system that leaves only isolated benzene subunits behind for stabilization of the electron on the fullerene (i.e., pristine $C_{60}$ versus hexakisadduct). In terms of storing excited-state energy, the high-lying level of the fullerene π-radical anion in $T_h$-hexakisadducts implies a net gain of nearly 0.7 eV in comparison with the monoadduct.

Based on the chemistry of the terminal groups and the highly symmetric three-dimensional architectures, even higher generation dendrimers derived from **7** and **19** can be envisioned. Since the core retains some of $C_{60}$'s electron- and energy-acceptor features and is also sufficiently shielded from the surrounding medium, several useful features might be realized, such as energy collection/transduction and amplification of electron transfer. For example, while evidence for dialkoxyanthracene moieties in **19** can be seen sufficiently in the UV and near-visible part of the spectrum, further extension into the visible and near-infrared section will constitute the next design step. Furthermore, their ability to function as hosts for a range of ions and molecules points to its unique versatility for practical applications: π–π association with the fullerene core and weak van der Waals forces are realistic possibilities for facilitating trapping or encapsulating suitable guests within the interior of the higher generation systems. Currently, we are intensifying our research to explore these issues.

## Experimental Section

**General**: Picosecond laser flash photolysis experiments were carried out with 355 nm laser pulses from a mode-locked, Q-switched Quantel YG-501

DP Nd:YAG laser system (pulse width 18 ps, 2 – 3 mJ pulse$^{-1}$). Nanosecond laser studies were performed with laser pulses from a Molectron UV-400 nitrogen laser system (337.1 nm, 8 ns pulse width, 1 mJ pulse$^{-1}$). The photomultiplier output was digitized with a Tektronix 7912 AD programmable digitizer.

Pulse radiolysis experiments were performed by utilizing 50 ns pulses of 8 MeV electrons from a Model TB-8/16-1S Electron Linear Accelerator. Dosimetry was based on the oxidation of $SCN^-$ to $(SCN)_2^{\bullet-}$, which in aqueous, $N_2O$-saturated solutions takes place with $G = 0.6$ μM per joule of absorbed energy. The radical concentration generated per pulse amounted to (1 – 3) μM for all the systems investigated in this study.

Fluorescence lifetimes were measured with a Laser Strope Fluorescence Lifetime Spectrometer (Photon Technology International) with 337 nm laser pulses from a nitrogen laser fiber-coupled to a lens-based T-formal sample compartment equipped with a stroboscopic detector. Details of the Laser Strobe systems are described on the manufacturer's web site, http://www.pti-nj.com.

Emission spectra were recorded with a SLM 8100 Spectrofluorometer. The experiments were performed at room temperature. Each spectrum represents an average of at least five individual scans, and appropriate corrections were applied whenever necessary.

$^1$H NMR and $^{13}$C NMR: Jeol JNM EX 400 and Jeol JNM GX 400; MS: Varian Mat 311 A (EI) and Finnigan MAT 900 (FAB); FT IR: Bruker Vector 22; UV/Vis: Shimadzu UV 3102 PC; analytical HPLC: Shimadsu Sil 10 A, SPD 10 A, CBM 10 A, LC 10 ATFRC 10 A; preparative HPLC: Shimadsu Sil 10 A, SPD 10 A, CBM 10 A, LC 8 A, FRC 10 A; TLC: Macherey-Nagel, Alugram Sil G/UV254. Reagents used were commercially available reagent grade and were purified according to standard procedures.

**Cyclic malonates 1, 4, and 5**: A solution of diol **3** (1.14 g, 4.5 mM) in dry dichloromethane (300 mL) was stirred, and a solution of malonyl dichloride (650 mg, 4.5 mM) was added dropwise over 16 hours under a nitrogen atmosphere. Afterwards the solvent was removed under reduced pressure. Separation and purification of the products were achieved by flash chromatography (toluene/triethylamine 19:1) followed by preparative HPLC (Gromsil-Amino-Phase, toluene).

*Yields*: **1**: 150 mg (0.47 mM, 10 %) colorless oil; **4**: 250 mg (0.39 mM, 16 %), colorless oil; **5**: 50 mg (0.05 mM, 3 %), slightly yellow oil.

*Compound* ***1***: $^1$H NMR (400 MHz, $CDCl_3$, 25 °C): $\delta = 1.83$ (m, 4H; $CH_2$), 2.70 (s, 6H; $CH_3$), 3.24 (t, $J = 6.9$ Hz, 4H; $CH_2$), 3.28 (s, 2H; $CH_2$), 4.11 (t, $J = 5.4$ Hz, 4H; $CH_2$), 6.92 (s, 4H; CH); $^{13}$C NMR (100.50 MHz, $CDCl_3$, 25 °C): $\delta = 25.52$ (2C; $CH_2$), 39.46 (2C; $CH_3$), 42.32 (1C; O=$CCH_2$C=O), 49.32 (2C; $CH_2$), 63.21 (2C; $CH_2$), 119.84 (2C; CH), 122.46 (2C; CH), 145.57 (2C; C), 166.36 (2C; C=O); MS (FAB): *m*/*z* (%): 320 $[M]^+$; IR (film): $\tilde{\nu} = 3057$, 2958, 2845, 2798, 1733, 1590, 1495, 1452, 1415, 1382, 1304, 1266, 1185, 1128, 1064, 1035, 988, 960, 887, 751, 683 cm$^{-1}$; UV/Vis ($CH_2Cl_2$): $\lambda_{max}$ ($\varepsilon$) = 239 (33000), 267 nm (5700).

*Compound* ***4***: $^1$H NMR (400 MHz, $CDCl_3$, 25 °C): $\delta = 1.83$ (m, 8H; $CH_2$), 2.71 (s, 12H; $CH_3$), 3.14 (t, $J = 7.2$ Hz, 8H; $CH_2$), 3.32 (s, 4H; $CH_2$), 4.14 (t, $J = 6.5$ Hz, 8H; $CH_2$), 6.92 (s, 8H; CH); $^{13}$C NMR (100.50 MHz, $CDCl_3$, 25 °C): $\delta = 26.01$ (4C; $CH_2$), 39.73 (4C; $CH_3$), 41.41 (2C; O=$CCH_2$C=O), 50.33 (4C; $CH_2$), 63.99 (4C; $CH_2$), 119.60 (4C; CH), 122.40 (4C; CH), 145.40 (4C; C), 166.56 (4C; C=O); MS (FAB): *m*/*z* (%): 642 $[M+H]^+$; IR (film): $\tilde{\nu} = 3057$, 2956, 2844, 2799, 1733, 1590, 1495, 1452, 1413, 1385, 1334, 1272, 1185, 1098, 1056, 1037, 958, 887, 752 cm$^{-1}$; UV/Vis ($CH_2Cl_2$): $\lambda_{max}$ ($\varepsilon$) = 238 nm (24000), 268 (12000).

*Compound* ***5***: $^1$H NMR (400 MHz, $CDCl_3$, 25 °C): $\delta = 1.81$ (m, 12H; $CH_2$), 2.72 (s, 18H; $CH_3$), 3.14 (t, $J = 7.1$ Hz, 12H; $CH_2$), 3.32 (s, 6H; $CH_2$), 4.14 (t, $J = 6.6$ Hz, 12H; $CH_2$), 6.91 (s, 12H; CH); $^{13}$C NMR (100.50 MHz, $CDCl_3$, 25 °C): $\delta = 26.03$ (6C; $CH_2$), 39.74 (6C; $CH_3$), 41.39 (3C; O=$CCH_2$C=O), 50.16 (6C; $CH_2$), 63.98 (6C; $CH_2$), 119.59 (6C; CH), 122.36 (6C; CH), 145.24 (6C; C), 166.50 (6C; C=O); MS (FAB): *m*/*z* (%): 962 $[M+H]^+$; IR (film): $\tilde{\nu} = 3057$, 2957, 2845, 2800, 1733, 1590, 1495, 1455, 1413, 1385, 1272, 1185, 1098, 1037, 957, 752, 687 cm$^{-1}$; UV/Vis ($CH_2Cl_2$): $\lambda_{max}$ ($\varepsilon$) = 238 (33000), 268 nm (17000).

**Monoadduct 6**: The diamine **1** (110 mg, 0.34 mM), tetrabromomethane (115 mg, 0.34 mM), and DBU (65 mg, 0.42 mM) were added to a solution of $C_{60}$ (190 mg, 0.26 mM) in pure toluene (130 mL) under a nitrogen atmosphere. After stirring overnight the mixture was filtered, and the product was separated by flash chromatography (toluene/ethyl acetate 16:1). Yield: 60 mg (0.06 mM, 23 %), red brownish solid.

$^1$H NMR (400 MHz, $CDCl_3$, 25 °C): $\delta = 2.05$ (m, 4H; $CH_2$), 2.81 (s, 6H; $CH_3$), 3.45 (t, $J = 6.6$ Hz, 4H; $CH_2$), 4.44 (t, $J = 5.4$ Hz, 4H; $CH_2$), 6.99 (m, 4H; CH); $^{13}$C NMR (100.50 MHz, $CDCl_3$, 25 °C): $\delta = 25.41$ (2C; $CH_2$), 39.69 (2C; $CH_3$), 49.18 (2C; $CH_2$), 51.95 (1C; bh; bridge head–C), 65.09 (2C; $CH_2$), 71.50 (2C; $sp^3$-$C_{60}$ C), 119.99 (2C; CH), 122.77 (2C; CH), 139.06, 140.94, 141.93, 142.20, 143.01, 143.06, 143.89, 144.60, 144.69, 144.87, 145.16, 145.26, 145.49 ($sp^2$ C), 163.53 (2C; C=O); MS (FAB): *m*/*z* (%): 1039 $[M]^+$; IR (KBr): $\tilde{\nu} = 3059$, 2951, 2925, 2841, 2794, 1744, 1494, 1449, 1428, 1267, 1232, 1203, 1186, 1056, 906, 803, 730 cm$^{-1}$; UV/Vis ($CH_2Cl_2$): $\lambda_{max}$ ($\varepsilon$) = 258 (115000), 326 (33000), 426 (2200), 486 nm (1400).

**Hexakisadduct 7**: Compound 9,10-dimethylanthracene (86 mg, 0.42 mM) was added to a solution of $C_{60}$ (30 mg, 0.042 mM) in pure toluene (50 mL) under a nitrogen atmosphere, and the mixture was stirred for three hours. Then diamine **1** (133 mg, 0.42 mM), tetrabromomethane (138 mg, 0.42 mM), and DBU (84 mg, 0.55 mM) were added. After stirring over night the mixture was filtered. Separation and purification of the product was achieved by flash chromatography (toluene/triethylamine 19:1) followed by preparative HPLC (Gromsil-Amino-Phase, toluene). Yield: 13 mg (0.005 mM, 12 %), yellow solid.

$^1$H NMR (400 MHz, $CDCl_3$, 25 °C): $\delta = 1.90$ (m, 24H; $CH_2$), 2.72 (s, 36H; $CH_3$), 3.29 (t, $J = 6.2$ Hz, 24H; $CH_3$), 4.16 (t, $J = 5.2$ Hz, 24H; $CH_2$), 6.93 (m, 24H; CH); $^{13}$C NMR (100.50 MHz, $CDCl_3$, 25 °C): $\delta = 25.33$ (12C; $CH_2$), 39.73 (12C; $CH_3$), 45.21 (6C; Bk–C), 49.21 (12C; $CH_2$), 64.78 (12C; $CH_2$), 68.96 (12C; $sp^3$-$C_{60}$ C), 119.93 (12C; CH), 122.66 (12C; CH), 140.94 (24C; $sp^2$ C), 145.49 (12C; C), 145.70 (24C; $sp^2$-C), 163.62 (12C; C=O); MS (FAB): *m*/*z* (%): 2630 $[M]^+$, 1316; IR (KBr): $\tilde{\nu} = 3056$, 2956, 2844, 2797, 1746, 1590, 1495, 1451, 1265, 1210, 1125, 1062, 750, 715 cm$^{-1}$; UV/Vis ($CH_2Cl_2$): $\lambda_{max}$ ($\varepsilon$) = 240 (141000), 270 (92000), 334 nm (34000).

**9,10-Bis(3-hydroxypropoxy)anthracene 8**: Nitrogen-saturated water (200 mL) and pure dichloromethane (200 mL) were added to a mixture of 9,10-anthraquinone (4.16 g, 20 mM), sodium dithionite (85 %, 8.2 g, 40 mM), and Adogen 464 (methyltrialkyl (C8-C10) ammonium chloride) (7.4 g, 16 mmol), and the mixture was stirred for 5 minutes. Then sodium hydroxide (8.0 g, 200 mM) was added, and stirring was continued for 10 minutes, and the mixture turned dark red. Compound 3-iodopropanol (18.2 g, 100 mM) was added dropwise, and the mixture was stirred for 16 hours at room temperature. The phases were separated, and the aqueous phase was washed with dichloromethane (2 × 200 mL). The organic phases were combined, washed with water (2 × 100 mL), and dried over magnesium sulfate. The filtrate was reduced to 100 mL, and the product was precipitated at −25 °C. Further purification of the crude product was achieved by flash chromatography (silica gel, dichloromethane/ethyl acetate 3:1). Yield: 2.1 g (6.4 mM, 32 %), yellow solid, melting point 148 °C.

$^1$H NMR (400 MHz, [$D_6$]DMSO, 25 °C): $\delta = 2.12$ (m, 2H; $CH_2$), 3.78 (q, $J = 5.5$ Hz, 2H; $OCH_2$), 4.19 (t, $J = 6.3$ Hz, 2H; $OCH_2$), 4.66 (t, $J = 5.2$ Hz, 2H; OH), 7.54 (m, 4H; CH), 8.27 (m, 4H; CH); $^{13}$C NMR (100 MHz, [$D_6$]DMSO, 25 °C): $\delta = 33.23$ (2C; $CH_2$), 57.43 (2C; $OCH_2$), 72.82 (2C; $OCH_2$), 122.41 (4C; arom. C), 124.53 (4C; arom. C), 125.58 (4C; arom. C), 146.80 (2C; arom. C); MS (FAB): *m*/*z* (%): 326 $[M]^+$, 267, 209, 152; IR (KBr): $\tilde{\nu} = 3313$, 3068, 3053, 3038, 2927, 2875, 1654, 1522, 1518, 1434, 1424, 1402, 1368, 1344, 1169, 1091, 1067, 973, 936, 778, 754, 676, 608 cm$^{-1}$; UV/Vis ($CH_2Cl_2$): $\lambda_{max}$ ($\varepsilon$) = 262 (82000), 366 (3700), 384 (5500), 406 nm (4800).

**Cyclic malonates 9 and 10**: Diol **8** (1.2 g, 3.7 mM) was dissolved in dry dichloromethane (500 mL) under a nitrogen atmosphere. A solution of malonyl dichloride (540 mg, 3.7 mM) in dry dichloromethane (300 mL) was added dropwise over 24 hours. The reaction was controlled by TLC (dichloromethane/ethyl acetate 19:1). Separation of the products was achieved by flash chromatography with gradient elution (silica gel, dichloromethane/ethyl acetate 19:1 – 9:1). The separated products were washed with pentane and dried in a vacuum.

*Yields*: **9**: 50 mg (0.38 mM, 10 %), yellow solid, melting point 288 °C; **10**: 200 mg (0.25 mM, 13 %), yellow solid, melting point: 193 °C.

*Compound* ***9***: $^1$H NMR (400 MHz, $CDCl_3$, 25 °C): $\delta = 2.06$ (m, 4H; $CH_2$), 2.53 (s, 2H; $OCCH_2CO$), 3.83 (t, $J = 6.0$ Hz, 4H; $CH_2OC$=O), 4.54 (t, $J = 6.0$ Hz, 4H; $OCH_2$), 7.44 (m, 4H; arom. H), 8.25 (m, 4H; arom. H); $^{13}$C NMR (100 MHz, $CDCl_3$, 25 °C): $\delta = 29.63$ (2C; $CH_2$), 40.68 (1C; $OCCH_2CO$), 61.74 (2C; $CH_2OC$=O), 72.23 (2C; $OCH_2$), 122.80 (4C; CH), 124.46 (4C; C), 125.05 (4C; CH), 147.65 (2C; C), 165.44 (2C; C=O); MS



0947-6539/02/0804-0988 $ 17.50+.50/0 *Chem. Eur. J.* **2002**, *8*, No. 4

(FAB): *m/z* (%): 394 $[M]^+$; IR (KBr): $\tilde{\nu}$ = 3065, 3049, 2960, 2894, 1743, 1676, 1618, 1462, 1436, 1407, 1380, 1361, 1348, 1331, 1283, 1187, 1171, 1154, 1129, 1084, 1059, 995, 930, 781, 689 cm$^{-1}$; UV/Vis ($CH_2Cl_2$): $\lambda_{max}$ ($\varepsilon$) = 264 (106000), 372 (5000), 390 (5900), 410 (5000).

*Compound* ***10***: $^1$H NMR (400 MHz, $CDCl_3$, 25 °C): $\delta$ = 2.13 (m, 8H; $CH_2$), 3.50 (s, 4H; $OCCH_2CO$), 3.87 (t, $J$ = 6.1 Hz, 8H; $CH_2OC$=O), 4.43 (t, $J$ = 6.2 Hz, 8H; $OCH_2$), 7.32 (m, 8H; arom. CH), 8.01 (m, 8H; arom. CH); $^{13}$C NMR (100 MHz, $CDCl_3$, 25 °C): $\delta$ = 29.42 (4C; $CH_2$), 42.01 (2C; $OCCH_2CO$), 62.58 (4C; $CH_2OC$=O), 71.54 (4C; $OCH_2$), 122.27 (8C; CH), 124.78 (8C; C), 125.34 (8C; CH), 146.92 (4C; C), 166.30 (4C; C=O); MS (FAB): *m/z* (%): 788 $[M]^+$; IR (KBr): $\tilde{\nu}$ = 3069, 2966, 2928, 2881, 1758, 1729, 1620, 1476, 1458, 1436, 1407, 1387, 1364, 1348, 1324, 1304, 1275, 1223, 1215, 1160, 1109, 1087, 1069, 1044, 1018, 980, 940, 892, 861, 853, 779, 764, 752 cm$^{-1}$; UV/Vis ($CH_2Cl_2$): $\lambda_{max}$ ($\varepsilon$) = 254 (145000), 262 (173000), 350 (5100), 366 (10000), 384 (14900), 406 nm (12700).

**1-{3-[(10-{3-[(3-Methoxy-3-oxopropanoyl)oxy]propoxy}-9-anthryl)oxy]-propyl}3-methylmalonate 11**: Methyl malonyl chloride (169 mg, 1.22 mM) was added dropwise to a solution of diol **8** (200 mg, 0.61 mM) and pyridine (100 mg, 1.22 mM) in dry dichloromethane (100 mL) under a nitrogen atmosphere. The mixture was stirred at room temperature for two hours, and the progress of the reaction was monitored by TLC. The product was isolated by flash chromatography (silica gel, dichloromethane/ethyl acetate 19:1) and dried in a vacuum. Yield: 230 mg, (0.44 mM, 72%), yellow solid, melting point 79 °C.

$^1$H NMR (400 MHz, $CDCl_3$, 25 °C): $\delta$ = 2.39 (m, $J$ = 6.4 Hz, 4H; $CH_2$), 3.46 (s, 4H; $CH_2$), 3.69 (s, 6H; $CH_3$), 4.24 (t, $J$ = 6.4 Hz, 4H; $CH_2$), 4.63 (t, $J$ = 6.4 Hz, 4H; $CH_2$), 7.49 (m, 4H; CH), 8.23 (m, 4H; CH); $^{13}$C NMR (100 MHz, $CDCl_3$, 25 °C): $\delta$ = 29.63 (2C; $CH_2$), 41.40 (2C; O=$CCH_2$C=O), 52.53 (2C; $CH_3$), 62.56 (2C; $CH_2OC$=O), 71.78 (2C; $OCH_2$), 122.46 (4C; CH), 125.02 (4C; C), 125.46 (4C; CH), 147.15 (2C; Ph−C−O), 166.53 (2C; C=O), 166.90 (2C; C=O); MS (FAB): *m/z* (%): 526 $[M]^+$; IR (KBr): $\tilde{\nu}$ = 3062, 2996, 2961, 2936, 2884, 1753, 1677, 1617, 1437, 1407, 1347, 1286, 1194, 1155, 1066, 1018, 942, 784, 753, 676 cm$^{-1}$; UV/Vis ($CH_2Cl_2$): $\lambda_{max}$ ($\varepsilon$) = 262 (94000), 348 (2400), 364 (4100), 384 (6100), 405 nm (5300).

**Monoadduct 12**: DBU (29 mg, 0.19 mM) was added dropwise to a solution of $C_{60}$ (122 mg, 0.17 mM), bismalonate **11** (90 mg, 0.17 mM), and tetrabromomethane (57 mg, 0.17 mM) in dry toluene (100 mL) under a nitrogen atmosphere. The mixture was stirred at room temperature for 16 hours, and the progress of the reaction was monitored by TLC. The product was isolated by flash chromatography (silica gel, toluene/ethyl acetate 19:1). Finally, the product was washed with pentane, dried in a vacuum, and stored under nitrogen. Yield: 45 mg (0.036 mM, 21%), red brownish solid.

$^1$H NMR (400 MHz, $CDCl_3$, 25 °C): $\delta$ = 2.39 (m, 2H; $CH_2$), 2.60 (m, 2H; $CH_2$), 3.46 (s, 2H; $OCCH_2CO$), 3.70 (s, 3H; $CH_3$), 3.96 (s, 3H; $CH_3$), 4.24 (t, $J$ = 6.2 Hz, 2H; $OCH_2$), 4.35 (t, $J$ = 6.4 Hz, 2H; $OCH_2$), 4.63 (t, $J$ = 6.3 Hz, 2H; $OCH_2$), 4.98 (t, $J$ = 6.2 Hz, 2H; $OCH_2$), 7.50 (m, 4H; CH), 8.22 (m, 2H; CH), 8.30 (m, 2H; CH); $^{13}$C NMR (100 MHz, $CDCl_3$, 25 °C): $\delta$ = 29.63 (1C; $CH_2$), 29.81 (1C; $CH_2$), 41.37 (1C; $OCCH_2CO$), 52.02 (1C; Bk−C), 52.52 (1C; $CH_3$), 53.98 (1C; $CH_3$), 62.53 (1C; $CH_2OC$=O), 64.56 (1C; $CH_2OC$=O), 71.43, 71.81, 72.07 ($OCH_2$ + $C_{60}$-$sp^3$-C), 122.44 (2C; arom. CH), 122.49 (2C; arom. CH), 125.03 (4C; arom. C), 125.49 (2C; arom. CH), 125.65 (2C; arom. CH), 138.84, 139.08, 140.85, 140.89, 141.77, 141.90, 142.13, 142.17, 142.94, 142.99, 143.05, 143.80, 143.85, 144.52, 144.62, 144.65, 144.87, 144.98, 145.07, 145.11, 145.16, 145.20, 145.26 ($C_{60}$-$sp^2$-C), 147.10 (1C; ArC−O), 147.27 (1C; ArC−O), 163.58 (1C; C=O), 164.00 (1C; C=O), 166.50 (1C; C=O), 166.87 (1C; C=O); MS (FAB): *m/z* (%): 1244 $[M]^+$, 720; IR (KBr): $\tilde{\nu}$ = 2960, 1744, 1433, 1406, 1347, 1266, 1234, 1066, 803, 774, 702, 609 cm$^{-1}$; UV/Vis ($CH_2Cl_2$): $\lambda_{max}$ ($\varepsilon$) = 262 (199000), 326 (34000), 382 (12600), 405 (8500), 426 (2800), 489 (1800), 688 nm (400).

**Fullerene adducts 13, 14, 15, and 16**: [60]Fullerene (720 mg, 1.0 mM) was dissolved in pure toluene (400 mL) under a nitrogen atmosphere and under exclusion of light. Then, malonate **11** (526 mg, 1.0 mM) and tetrabromomethane (663 mg, 2.0 mM) were added. DBU (335 mg, 2.2 mM) was added slowly over 5 hours. The mixture was stirred for 20 hours, and the course of the reaction was monitored by TLC (silica gel, toluene/ethyl acetate 19:1). The mixture was reduced to 100 mL, and it was preselected by flash chromatography (silica gel, toluene/ethyl acetate 19:1). The separation of the products was achieved by preparative HPLC (nucleosil, toluene/ethyl acetate 99:1). The products were washed with pentane, dried in a vacuum, and stored under nitrogen.

*Yields*: **16**: 55 mg (0.028 mM, 3%, $T_R$ = 2.3 min), red brownish solid; **13**: 62 mg (0.048 mM, 5%, $T_R$ = 6.0 min), red brownish solid; **14**: 112 mg (0.090 mM, 9%, $T_R$ = 7.3 min), red brownish solid; **15**: 34 mg (0.027 mM, 3%, $T_R$ = 8.4 min), red brownish solid.

*Compound* ***16***: $^1$H NMR (400 MHz, $CDCl_3$, 25 °C): $\delta$ = 2.59 (m, 4H; $CH_2$), 3.97 (s, 6H; $CH_3$), 4.33 (t, $J$ = 6.2 Hz, 4H; $OCH_2$), 4.96 (t, $J$ = 6.0 Hz, 4H; $OCH_2$), 7.52 (m, 4H; CH), 8.27 (m, 4H; CH); $^{13}$C NMR (100 MHz, $CDCl_3$, 25 °C): $\delta$ = 29.58 (2C; $CH_2$), 51.78 (2C; Bk−C), 54.02 (2C; $CH_3$), 64.42 (2C; $CH_2OC$=O), 71.16 (4C; $C_{60}$-$sp^3$-C), 71.98 (2C; $OCH_2$), 122.22 (4C; arom. CH), 124.74 (4C; arom. C), 125.62 (4C; arom. CH), 138.48, 138.85, 140.57, 141.48, 141.59, 141.85, 142.63, 142.70, 142.78, 143.51, 143.58, 144.24, 144.31, 144.37, 144.59, 144.68, 144.75, 144.81, 144.84, 144.88 ($C_{60}$-$sp^2$-C), 146.91 (2C; ArC−O), 163.39 (2C; C=O), 163.81 (2C; C=O); MS (FAB): *m/z* (%): 1964 $[M+H]^+$, 720; IR (KBr): $\tilde{\nu}$ = 2924, 1744, 1636, 1430, 1266, 1235, 1186, 1062, 948, 888, 744, 704 cm$^{-1}$; UV/Vis ($CH_2Cl_2$): $\lambda_{max}$ ($\varepsilon$) = 262 (182000), 325 (46000), 403 (8800), 426 nm (4700).

*Compound* ***13***: $^1$H NMR (400 MHz, $CDCl_3$, 25 °C): $\delta$ = 2.53 (m, 4H; $CH_2$), 3.92 (m, 2H; $OCH_2$), 4.10 (m, 2H; $OCH_2$), 4.16 (s, 6H; $CH_3$), 4.47 (m, 2H; $OCH_2$), 4.97 (m, 2H; $OCH_2$), 7.26 (m, 2H; CH), 7.48 (m, 2H; CH), 7.93 (d, $J$ = 8.8 Hz, 2H; CH), 8.42 (d, $J$ = 8.8 Hz, 2H; CH); $^{13}$C NMR (100 MHz, $CDCl_3$, 25 °C): $\delta$ = 29.14 (2C; $CH_2$), 51.39 (2C; Bk−C), 54.06 (2C; $CH_3$), 64.61 (2C; $CH_2OC$=O), 70.79 (2C; $C_{60}$-$sp^3$-C), 71.17 (2C; $C_{60}$-$sp^3$-C), 74.36 ($OCH_2$), 122.19 (2C; arom. CH), 122.66 (2C; arom. CH), 124.59 (2C; arom. C), 124.84 (2C; arom. C), 125.48 (2C; arom. CH), 125.80 (2C; arom. CH), 137.32, 137.72, 139.30, 141.21, 141.51, 141.69, 142.18, 142.33, 142.45, 142.97, 143.21, 143.32, 143.67, 143.82, 144.26, 144.46, 144.84, 144.94, 145.32, 145.46, 145.56, 145.94, 146.14, 146.31, 146.38, 146.52, 146.73, 147.11 ($C_{60}$-$sp^2$-C), 148.01 (2C; ArC−O), 162.87 (2C; C=O), 163.90 (2C; C=O); MS (FAB): *m/z* (%): 1243 $[M+H]^+$, 720; IR (KBr): $\tilde{\nu}$ = 3065, 2960, 1748, 1435, 1366, 1349, 1260, 1228, 1102, 1063, 1031, 803, 757, 708 cm$^{-1}$; UV/Vis ($CH_2Cl_2$): $\lambda_{max}$ ($\varepsilon$) = 254 (117000), 262 (118000), 408 (5700), 488 nm (2300).

*Compound* ***14***: $^1$H NMR (400 MHz, $CDCl_3$, 25 °C): $\delta$ = 2.51 (m, 2H; $CH_2$), 2.62 (m, 1H; $CH_2$), 2.76 (m, 1H; $CH_2$), 3.76 (m, 1H; $OCH_2$), 3.96 (m, 1H; $OCH_2$), 4.09 (s, 3H; $CH_3$), 4.12 (s, 3H; $CH_3$), 4.17 (m, 1H; $OCH_2$), 4.33 (m, 1H; $OCH_2$), 4.42 (m, 1H; $OCH_2$), 4.63 (m, 1H; $OCH_2$), 4.90 (m, 1H; $OCH_2$), 5.17 (m, 1H; $OCH_2$), 7.23 (m, 2H; CH), 7.34 (m, 1H; CH), 7.47 (m, 1H; CH), 7.94 (d, $J$ = 8.8 Hz, 1H; CH), 8.02 (d, $J$ = 8.1 Hz, 1H; CH), 8.10 (d, $J$ = 8.1 Hz, 1H; CH), 8.58 (d, $J$ = 8.8 Hz, 1H; CH); $^{13}$C NMR (100 MHz, $CDCl_3$, 25 °C): $\delta$ = 29.19 (1C; $CH_2$), 29.42 (1C; $CH_2$), 51.51 (2C; bridgehead-C), 54.05 (2C; $CH_3$), 64.65 (1C; $CH_2OC$=O), 65.33 (1C; $CH_2OC$=O), 70.79, 70.88, 70.95 ($C_{60}$-$sp^3$-C), 73.16 (1C; $OCH_2$), 74.64 (1C; $OCH_2$), 122.07, 122.27, 123.20, 124.21, 124.85, 125.45, 125.54, 126.04 (arom. C), 136.56, 136.60, 137.95, 138.59, 140.05, 140.72, 140.82, 141.33, 141.64, 141.68, 141.77, 142.26, 142.81, 142.90, 143.19, 143.26, 143.37, 143.56, 143.72, 143.78, 143.85, 144.01, 144.14, 144.31, 144.54, 145.07, 145.18, 145.68, 145.73, 146.02, 146.13, 146.33, 146.41, 146.54, 146.86, 147.01, 147.12 ($C_{60}$-$sp^2$-C), 147.56, 147.61 (ArC−O), 162.67, 163.82, 163.96 (C=O); MS (FAB): *m/z* (%): 1243 $[M+H]^+$, 720; IR (KBr): $\tilde{\nu}$ = 3065, 2950, 2881, 1747, 1433, 1364, 1349, 1234, 1104, 1062, 1032, 756, 731, 708, 671 cm$^{-1}$; UV/Vis ($CH_2Cl_2$): $\lambda_{max}$ ($\varepsilon$) = 254 (139000), 262 (139000), 408 (6900), 486 nm (2600).

*Compound* ***15***: $^1$H NMR (400 MHz, $CDCl_3$, 25 °C): $\delta$ = 2.63 (m, 2H; $CH_2$), 2.74 (m, 2H; $CH_2$), 3.94 (m, 2H; $OCH_2$), 4.23 (s, 6H; $CH_3$), 4.26 (m, 2H; $OCH_2$), 4.57 (m, 2H; $OCH_2$), 4.91 (m, 2H; $OCH_2$), 7.33 (m, 4H; CH), 8.06 (m, 2H; CH), 8.16 (m, 2H; CH); $^{13}$C NMR (100 MHz, $CDCl_3$, 25 °C): $\delta$ = 29.49 (2C; $CH_2$), 50.24 (2C; bridgehead-C), 54.25 (2C; $CH_3$), 65.27 (2C; $CH_2OC$=O), 70.62 (2C; $C_{60}$-$sp^3$-C), 71.29 (2C; $C_{60}$-$sp^3$-C), 74.36 (2C; $OCH_2$), 122.55 (4C; arom. CH), 124.53 (2C; arom. C), 124.98 (2C; arom. C), 125.42 (2C; arom. CH), 125.76 (2C; arom. CH), 135.39, 135.61, 139.99, 140.86, 141.48, 141.63, 141.77, 142.07, 142.19, 142.50, 142.88, 143.14, 143.20, 143.47, 143.53, 143.91, 144.06, 144.29, 144.44, 144.68, 144.79, 145.09, 145.35, 145.43, 146.00, 146.26, 146.78, 146.88 ($C_{60}$-$sp^2$-C), 147.26 (2C; ArC−O), 164.26 (2C; C=O), 164.54 (2C; C=O); MS (FAB): *m/z* (%): 1243 $[M+H]^+$, 720; IR (KBr): $\tilde{\nu}$ = 3062, 3022, 2950, 2924, 2877, 1747, 1434, 1362, 1238, 1107, 1062, 1030, 776, 736, 702, 668 cm$^{-1}$; UV/Vis ($CH_2Cl_2$): $\lambda_{max}$ ($\varepsilon$) = 262 (150000), 383 (11900), 405 (7400), 430 (3100), 486 nm (2100).

**Monoadduct 17**: DBU (30 mg, 0.2 mM) was added dropwise to a solution of [60]fullerene (100 mg, 0.14 mM), malonate **9** (65 mg, 0.16 mM), and tetrabromomethane (55 mg, 0.16 mM) in pure toluene (100 mL) under a nitrogen atmosphere. The mixture was stirred for 16 hours, and the course of the reaction was monitored by TLC (silica gel, toluene/ethyl acetate

19:1). The product was isolated by flash chromatography (silica gel, toluene/ethyl acetate, 24:1), washed with pentane, and dried in a vacuum. Yield: 50 mg (0.045 mM, 32%), red brownish solid.

$^1$H NMR (400 MHz, $CDCl_3$, 25 °C): $\delta = 2.19$ (m, 4H; $CH_2$), 4.20 (t, $J = 6.0$ Hz, 4H; $CH_2OC{=}O$), 4.63 (t, $J = 5.9$ Hz, 4H; $OCH_2$), 7.44 (m, 4H; arom. H), 8.30 (m, 4H; arom. H); $^{13}$C NMR (100 MHz, $CDCl_3$, 25 °C): $\delta =$ 29.96 (2C; $CH_2$), 52.17 (1C; Bk–C), 63.35 (2C; $CH_2OC{=}O$), 71.10 ($C_{60}$-$sp^3$-C), 72.01 (2C; $OCH_2$), 122.75 (4C; CH), 124.52 (4C; CH), 125.49 (4C; CH), 138.26, 140.74, 141.73, 142.13, 142.86, 143.01, 143.80, 144.49, 144.54, 144.65, 144.84, 145.04, 145.18, 145.26 ($C_{60}$-$sp^2$-C), 147.92 (2C; ArC–O), 162.52 (2C; C=O); MS (FAB): $m/z$ (%): 1112 $[M]^+$, 720; IR (KBr): $\tilde{\nu} = 3047$, 2962, 1745, 1617, 1461, 1428, 1405, 1348, 1264, 1227, 1204, 1187, 1096, 1060, 928, 802, 780, 729, 684, 668 cm$^{-1}$; UV/Vis ($CH_2Cl_2$): $\lambda_{max}$ ($\varepsilon$) = 264 (176000), 326 (31000), 425 (3800), 494 (1300), 580 nm (600).

**Hexakisadduct 18**: Compound 9,10-dimethylanthracene (93 mg, 0.45 mM) was added to a solution of monoadduct **17** (50 mg, 0.045 mM) in pure toluene (50 mL) under a nitrogen atmosphere, and the mixture was stirred for 3 hours. Diethyl bromomalonate (107 mg, 0.45 mM) and DBU (68 mg, 0.45 mM) were then added. The mixture was stirred for 24 hours at room temperature, and the course of the reaction was monitored by analytical HPLC (nucleosil, toluene/ethyl acetate 19:1). The product was achieved by flash chromatography with gradient elution (silica gel, toluene/ethylacetate 19:1/9:1). It was washed with pentane and dried in a vacuum. Yield: 20 mg (0.011 mM, 23%), yellow orange solid.

$^1$H NMR (400 MHz, $CDCl_3$, 25 °C): $\delta = 1.29$ (m, 30H; $CH_3$), 1.92 (m, 4C; $CH_2$), 3.70 (t, $J = 6.3$ Hz, 4H; $OCH_2$), 4.29 (m, 20H; $OCH_2$), 4.52 (t, $J =$ 5.8 Hz, 4H; $OCH_2$), 7.47 (m, 4H; arom. H), 8.27 (m, 4H; arom. H); $^{13}$C NMR (100 MHz, $CDCl_3$, 25 °C): $\delta = 13.86$, 13.96, 14.07, 14.17 ($CH_3$), 29.43 (2C; $CH_2$), 45.02, 45.26 (Bk–C), 62.61, 62.82, 63.04, 63.35 ($OCH_2$), 68.73, 68.92, 68.96, 69.03 ($C_{60}$-$sp^3$-C), 71.73 (2C; $OCH_2$), 122.55, 122.63, 124.80, 125.44 (arom. C), 140.78, 140.96, 141.02, 141.07, 145.29, 145.61, 145.64, 145.68 ($C_{60}$-$sp^2$-C), 147.23, (2C; ArC–O), 162.66, 163.64, 163.75 (C=O); MS (FAB): $m/z$ (%): 1901 $[M]^+$; IR (KBr): $\tilde{\nu} = 3065$, 2979, 2937, 2905, 1745, 1465, 1368, 1350, 1219, 1079, 1018, 856, 715 cm$^{-1}$; UV/Vis ($CH_2Cl_2$): $\lambda_{max}$ ($\varepsilon$) = 246 (113000), 264 (165000), 281 (76000), 312 (47000), 334 (37000), 386 nm (10100).

**Hexakisadduct 19**: Compound 9,10-dimethylanthracene (79 mg, 0.38 mM) was added to a solution of $C_{60}$ (27 mg, 0.038 mM) in pure toluene (50 mL) under a nitrogen atmosphere, and the mixture was stirred for 3 hours. Malonate **9** (150 mg, 0.38 mM), tetrabromomethane (126 mg, 0.38 mM), and DBU (73 mg, 0.48 mM) were then added. The mixture was stirred for 48 hours at room temperature, and the course of the reaction was monitored by TLC (nucleosil, toluene/ethyl acetate 19:1). The product was obtained by flash chromatography (silica gel, toluene/ethylacetate 19:1) followed by preparative HPLC (nucleosil, dichloromethane/ethanol, 99.7:0.3). It was then washed with pentane and dried in a vacuum. Yield: 10 mg (0.003 mM, 9%), yellow solid.

$^1$H NMR (400 MHz, $C_2D_2Cl_4$, 80 °C): $\delta = 1.83$ (br s, 24H; $CH_2$), 3.59 (br s, 24H; $OCCH_2CO$), 4.47 (br s, 24H; $OCH_2$), 7.48 (m, 24H; arom. H), 8.26 (m, 24H; arom. H); $^{13}$C NMR (100 MHz, $C_2D_2Cl_4$, 80 °C): $\delta = 29.07$ (12C; $CH_2$), 44.92 (6C; Bk–C), 63.54 (12C; $OCCH_2CO$), 68.48 (12C; $C_{60}$-$sp^3$-C), 71.23 (12C; $OCH_2$), 122.35 (24C; CH), 124.75 (24C; C), 125.31 (24C; CH), 140.26 (24C; $C_{60}$-$sp^2$-C), 144.60 (24C; $C_{60}$-$sp^2$-C), 146.72 (12C; ArC–O), 162.11 (12C; C=O); MS (FAB): $m/z$ (%): 3073 $[M]^+$; IR (KBr): $\tilde{\nu} = 3065$, 2959, 1745, 1618, 1406, 1349, 1263, 1212, 1053, 781, 715, 687, 665 cm$^{-1}$; UV/Vis ($CH_2Cl_2$): $\lambda_{max}$ ($\varepsilon$) = 264 (198000), 370 (10200), 389 (11000), 411 (8800), 524 nm (900).

## Acknowledgements

Part of this work was supported by the Office of Basic Energy Sciences of the US Department of Energy. This is document NDRL-XXXX from the Notre Dame Radiation Laboratory. We thank the Deutsche Forschungsgemeinschaft (DFG) and the Stiftung Volkswagenwerk for financial support.

[1] a) F. Diederich, R. Kessinger, *Acc. Chem. Res.* **1999**, *32*, 537; b) F. Diederich, M. Gomez-Lopez, *Chem. Soc. Rev.* **1999**, *28*, 263; c) M. Hetzer, H. Clausen-Schaumann, S. Bayerl, T. M. Bayerl, X. Camps, O. Vostrowsky, A. Hirsch, *Angew. Chem.* **1999**, *111*, 2103; *Angew. Chem. Int. Ed.* **1999**, *38*, 1962; d) F. Djojo, E. Ravanelli, A. Hirsch, O. Vostrowsky, *Eur. J. Org. Chem.* **2000**, 1051; e) M. Brettreich, S. Burghardt, C. Böttcher, S. Bayerl, T. Bayerl, A. Hirsch, *Angew. Chem.* **2000**, *112*, 1915; *Angew. Chem. Int. Ed.* **2000**, *39*, 1845; f) M. Braun, X. Camps, O. Vostrowsky, A. Hirsch, E. Endreß, T. M. Bayerl, O. Birkert, G. Gauglitz, *Eur. J. Org. Chem.* **2000**, 1173; g) J. F. Nierengarten, *Chem. Eur. J.* **2000**, *6*, 3667.

[2] a) H. Imahori, Y. Sakata, *Adv. Mater.* **1997**, *9*, 537; b) N. Martín, L. Sánchez, B. Illescas, I. Pérez, *Chem. Rev.* **1998**, *98*, 2527; c) H. Imahori, Y. Sakata, *Eur. J. Org. Chem.* **1999**, 2445; d) D. M. Guldi, *Chem. Commun.* **2000**, 321; e) D. M. Guldi, M. Prato, *Acc. Chem. Res.* **2000**, *33*, 695; f) S. Fukuzumi, D. M. Guldi in *Electron Transfer in Chemistry*, *Vol. 2* (Ed.: V. Balzani), Wiley-VCH, Weinheim, **2001**, p. 270.

[3] H. Imahori, D. M. Guldi, K. Tamaki, Y. Yoshida, C. Luo, Y. Sakata, S. Fukuzumi, *J. Am. Chem. Soc.* **2001**, *123*, 6617.

[4] a) N. S. Sariciftci, L. Smilowitz, A. J. Heeger, F. Wudl, *Science* **1992**, *258*, 1474; b) J.-F. Eckert, J.-F. Nicoud, J.-F. Nierengarten, S. G. Liu, N. Armaroli, L. Ouali, V. Krasnikov, G. Hadziioannou, *J. Am. Chem. Soc.* **2000**, *122*, 7467; c) C. Luo, D. M. Guldi, M. Maggini, E. Menna, S. Mondini, N. A. Kotov, M. Prato, *Angew. Chem.* **2000**, *112*, 4052; *Angew. Chem. Int. Ed.* **2000**, *39*, 3905; d) H. Imahori, H. Norieda, H. Yamada, Y. Nishimura, I. Yamazaki, Y. Sakata, S. Fukuzumi, *J. Am. Chem. Soc.* **2001**, *123*, 100; e) A. M. Ramos, M. T. Rispens, J. K. J. van Duren, J. C. Hummelen, R. A. J. Janssen, *J. Am. Chem. Soc.* **2001**, *123*, 6714.

[5] L. Echegoyen, L. E. Echegoyen, *Acc. Chem. Res.* **1998**, *31*, 593.

[6] a) P. J. Fagan, J. C. Calabrese, B. Malone, *J. Am. Chem. Soc.* **1991**, *113*, 9408; b) A. Hirsch, I. Lamparth, T. Gösser, H. R. Karfunkel, *J. Am. Chem. Soc.* **1994**, *116*, 9385; c) R. Schwenniger, T. Müller, B. Kräutler, *J. Am. Chem. Soc.* **1997**, *119*, 9317; d) L. Isaacs, F. Diederich, R. F. Haldimann, *Helv. Chim. Acta* **1997**, *80*, 317; e) W. Qian, Y. Rubin, *Angew. Chem.* **1999**, *111*, 2504; *Angew. Chem. Int. Ed.* **1999**, *38*, 2356; f) G. Schick, M. Levitus, L. Kvetko, B. A. Johnson, I. Lamparth, R. Lunkwitz, B. Ma, S. I. Khan, M. A. Garcia-Garibay, Y. Rubin, *J. Am. Chem. Soc.* **1999**, *121*, 3246; g) C. R. Woods, J.-P. Bourgeois, P. Seiler, F. Diederich, *Angew. Chem.* **2000**, *112*, 3971; *Angew. Chem. Int. Ed.* **2000**, *39*, 3813.

[7] a) D. K. Smith, F. Diederich, *Chem. Eur. J.* **1998**, *4*, 1353; b) M. Fischer, F. Vögtle, *Angew. Chem.* **1999**, *111*, 934; *Angew. Chem. Int. Ed.* **1999**, *38*, 884; c) R. M. Crooks, M. Zhao, L. Sun, V. Chechik, L. K. Yeung, *Acc. Chem. Res.* **2001**, *34*, 181; d) C. B. Gorman, J. C. Smith, *Acc. Chem. Res.* **2001**, *34*, 60.

[8] K. Bauer, U. Nickel, M. Diekers, A. Hirsch, unpublished results.

[9] a) I. Lamparth, C. Maichle-Mössmer, A. Hirsch, *Angew. Chem.* **1995**, *107*, 1755; *Angew. Chem. Int. Ed. Engl.* **1995**, *34*, 1607; b) A. Hirsch, O. Vostrowsky, *Eur. J. Org. Chem.* **2001**, 829.

[10] G. W. H. Cheeseman, *J. Chem. Soc.* **1955**, 3308.

[11] E. P. Kyba, R. E. Davis, C. W. Hudson, A. M. John, S. B. Brown, M. J. McPaul, L.-K. Liu, A. C. Glover, *J. Am. Chem. Soc.* **1981**, *103*, 3838.

[12] M. Diekers, A. Hirsch, C. Luo, D. M. Guldi, K. Bauer, U. Nickel, *Org. Lett.* **2000**, 2741.

[13] U. Seitz, J. Daub, *Synthesis* **1986**, 686.

[14] F. Djojo, A. Herzog, I. Lamparth, F. Hampel, A. Hirsch, *Chem. Eur. J.* **1996**, *2*, 1537.

[15] a) X. Camps, E. Dietel, A. Hirsch, S. Pyo, L. Echegoyen, S. Hackbarth, B. Roder, *Chem. Eur. J.* **1999**, *5*, 2362; b) C. Boudon, J.-P. Gisselbrecht, M. Gross, L. Isaacs, H. L. Anderson, R. Faust, F. Diederich, *Helv. Chim. Acta*, **1995**, *78*, 1334.

[16] The absorption spectra of the investigated donor–acceptor ensembles reveal the superimposed features of the individual components.

[17] D. M. Guldi, K.-D. Asmus, *J. Phys. Chem. A* **1997**, *101*, 1472.

[18] The fluorescence decay curves, which were well fitted by a single exponential decay component, further corroborate the steady-state experiments. Table 1 lists the respective fluorescence lifetimes in solvents of different polarity.

[19] S. L. Murov, I. Carmichael, G. L. Hug, *Handbook of Photochemistry*, Marcel Dekker, New York, **1993**.

[20] Pulse radiolytic reduction with $T_h$-$C_{66}$(COOEt)$_2$ was performed in oxygen-free 2-propanol, in which the solvated electron is the reducing entity.

[21] a) R. A. Marcus, *Annu. Rev. Phys. Chem.* **1964**, *15*, 155; b) R. A. Marcus, *Angew. Chem.* **1993**, *105*, 1161; *Angew. Chem. Int. Ed. Engl.* **1993**, *32*, 1111.

[22] a) R. J. Harrison, B. Pearce, G. S. Beddard, J. A. Cowan, J. K. M. Sanders, *Chem. Phys.* **1987**, *116*, 429; b) T. Asahi, M. Ohkohchi, R. Matsusaka, N. Mataga, R. P. Zhang, A. Osuka, K. Maruyama, *J. Am. Chem. Soc.* **1993**, *115*, 5665; c) A. Harriman, V. Heitz, J.-P. Sauvage, *J. Phys. Chem.* **1993**, *97*, 5940; d) L. R. Khundkar, J. W. Perry, J. E. Hanson, P. B. Dervan, *J. Am. Chem. Soc.* **1994**, *116*, 9700; e) H. Heitele, F. Pöllinger, T. Häberle, M. E. Michel-Beyerle, H. A. Staab, *J. Phys. Chem.* **1994**, *98*, 7402; f) A. N. Macpherson, P. A. Liddell, S. Lin, L. Noss, G. R. Seely, J. M. DeGraziano, A. L. Moore, T. A. Moore, D. Gust, *J. Am. Chem. Soc.* **1995**, *117*, 7202; g) A. Osuka, G. Noya, S. Taniguchi, T. Okada, Y. Nishimura, I. Yamazaki, N. Mataga, *Chem. Eur. J.* **2000**, *6*, 33.

[23] H. Imahori, K. Tamaki, D. M. Guldi, C. Luo, M. Fujitsuka, O. Ito, Y. Sakata, S. Fukuzumi, *J. Am. Chem. Soc.* **2001**, *123*, 2607.

[24] a) S. I. van Dijk, C. P. Groen, F. Hartl, A. Brouwer, J. W. Verhoeven, *J. Am. Chem. Soc.* **1996**, *118*, 8425; b) F. Hauke, A. Hirsch, S.-G, Liu, L. Echegoyen, A. Swartz, C. Luo, D. M. Guldi, *ChemPhysChem*. **2002**, *3*, in press.

Received: July 3, 2001 [F3388]

  0947-6539/02/0804-0991 $ 17.50+.50/0 